Landscape Ecology

https://doi.org/10.1007/s10980-026-02392-1

Article in Press

Integrating earth observation and graph theory to evaluate urban green spaces connectivity across European capitals

Received: 02 Dec 2025

Accepted: 31 May 2026

Costanza Borghi, Saverio Francini, Leonardo Chiesi, Stefano Mancuso, Liubov Tupikina, Guido Caldarelli, Jacopo Moi, Elia Vangi, Giovanni D'Amico, Giuseppe Luca & Gherardo Chirici

Cite this article as: Borghi, C., Francini, S., Chiesi, L. *et al.* Integrating earth observation and graph theory to evaluate urban green spaces connectivity across European capitals. *Landsc Ecol* (2026). https://doi.org/10.1007/s10980-026-02392-1

Integrating Earth Observation and Graph Theory to Evaluate Urban Green Spaces Connectivity Across European Capitals

Costanza Borghi[1,2], Saverio Francini[3*], Leonardo Chiesi[4,5], Stefano Mancuso[1], Liubov Tupikina[6,7], Guido Caldarelli[8,9,10,11], Jacopo Moi[8], Elia Vangi[1], Giovanni D'Amico[1], Giuseppe De Luca[12], Gherardo Chirici[1,2]

[1] Department of Agriculture, Food, Environment and Forestry (DAGRI), University of Florence, 50145 Florence, Italy

[2] Fondazione per il Futuro delle Città (FFC), Rome, Italy

[3] Department of Science and Technology of Agriculture and Environment (DISTAL), University of Bologna, 40126 Bologna, Italy

[4] Department of Political and Social Sciences (DSPS), University of Florence, 50100, Florence, Italy

[5] Department of System Design Engineering, Keio University, Yokohama, Japan

[6] Learning Planet Institute, F-75004, Paris, France

[7] Nokia Bell Labs, France

[8] National Research Council – Institute for Complex Systems (CNR - ISC), Rome, Italy

[9] Department of Molecular Sciences and Nanosystems (DSMN), Ca'Foscari University of Venice, Venice, Italy.

[10] European Centre for Living Technology (ECLT), Venice, Italy.

[11] London Institute for Mathematical Sciences (LIMS), London, UK.

[12] Department of Architecture (DIDA), University of Florence, 50100, Florence, Italy

* corresponding author *saverio.francini@unibo.it*

Acknowledgements

This article was carried out in the framework of the URBANA project, ESA Contract No. 4000143311/23/I-DT for "DEVELOPMENT AND VERIFICATION OF URBAN

ANALYTICS”, the LIFE ESCAPOS (Proposal number: 101157553) “Environment energy for Strategic CApillary urban POlicieS” and the “Advanced models for estimating carbon uptake by urban vegetation to support ecological transition policies” project, funded by the Tuscany Region under the initiative “Green Transition – Advanced Training Projects with Research Grants” (CUP B53C23002970009), within the European Social Fund Plus (ESF+) 2021–2027 Regional Programme – Priority 4 ‘Youth Employment.

The following projects also support the activities:

FORWARDS. H2020 project funded by the European Commission, number 101084481 call HORIZON-CL6-2022-CLIMATE-01-05.

MONIFUN. H2020 project funded by the European Commission, number 101134991 call HORIZON-CL6-2023-CircBio-01-14.

NextGenCarbon. H2020 project funded by the European Commission, number 101184989 call HORIZON-CL5-2024-D1-01-07.

SUPERB. H2020 project funded by the European Commission, number 101036849 call LC-GD-7-1-2020;

MULTIFOR “Multi-scale observations to predict Forest response to pollution and climate change” PRIN 2020 Research Project of National. Relevance funded by the Italian Ministry of University and Research (prot. 2020E52THS).

Abstract

Context

As global urbanization intensifies, Urban Green Spaces (UGS) are pivotal for biodiversity conservation and climate change mitigation. However, comparative assessments of UGS spatial configuration and connectivity across diverse urban landscapes remain limited.

Objectives

This study aims to assess the spatial arrangement and connectivity of UGS across 28 European capital cities. Additionally, we evaluate how Network Science metrics derived from Graph Theory can complement traditional landscape ecology metrics to provide a more comprehensive understanding of UGS at a large scale.

Methods

We developed a European Urban Vegetation Map using Earth observation data to classify UGS at 10 m resolution across the selected capitals. We then analyzed UGS connectivity for each city utilizing 40 traditional landscape metrics and a Graph-Theory-based approach.

Results

While traditional landscape metrics effectively quantified fragmentation, they often remain strongly correlated with total vegetation abundance. In contrast, Network Science metrics provided specific insights into UGS functional connectivity, distinguishing the quality of ecological links beyond spatial proximity. This integration allowed us to cluster European capitals into three distinct typologies: unconnected compact cities, large metropolises with complex peri-urban dynamics, and high-connectivity cities with robust networks. These findings demonstrate that graph-based indices effectively complement traditional metrics, highlighting that relying solely on green space coverage is insufficient for assessing the ecological resilience of urban environments.

Conclusions

These results underscore the relevance of Earth observation-based UGS assessment and demonstrate that graph-based landscape connectivity analysis outperforms simple abundance metrics. Therefore, effective assessment requires integrating structural metrics with graph-based connectivity to support resilient urban biodiversity.

Keywords: Urban Green Spaces, Connectivity, Landscape Ecology, Earth Observation, Graph Theory

1. Introduction

With the global population projected to reach about 10 billion in 2050 (Gu et al. 2021), almost 70% of the global population is expected to live in urban areas by the same year (United Nations 2018).

Urban Green Spaces (UGS) provide a vast range of ecosystem services (Stroud et al. 2022): carbon and pollutants removal (Han et al. 2024; Du et al. 2025), temperature regulation (Duncan et al. 2019), biodiversity conservation (Afrifa et al. 2022), and benefits to human mental and physical health (Konijnendijk 2023).

A standardized approach to assessing UGS is vital for supporting policymakers and urban planners in enhancing urban quality of life and building biodiverse, resilient cities (Norton et al. 2015). The European Union recognizes UGS in the Biodiversity Strategy for 2030 and within the objectives of the European Green Deal and the Sustainable Development Goals. However, their assessments often rely on an oversimplified indicator - the percentage of area covered by UGS (Maes et al. 2019). For example, the European Commission’s 2023 guidance for Nature Urban Plans prioritizes UGS percentage as the primary indicator, followed by tree cover and protected areas. This approach largely overlooks spatial arrangement, despite landscape ecology research emphasizing its functional importance (Turner and Gardner 2015; Herath et al. 2024). While the EU Regulation 2024/1991 on nature restoration represents a landmark step for urban ecosystems, its Article 8 continues to focus primarily on the sheer share of green space and tree canopy cover. Relying on such simplified, area-based metrics risks neglecting a fundamental ecological reality: the structural configuration of UGS is often more decisive for ecosystem services than their total extent alone. Indeed, monitoring the spatial arrangement of UGS in cities (Francini et al. 2024) is crucial for implementing nature-based solutions, limiting fragmentation and degradation (Huang et al. 2021), and assessing connectivity (Clauzel et al. 2018; Tarabon et al. 2022). Traditionally, this analysis implements landscape ecology metrics from categorical land-use/land-cover maps (Uuemaa et al. 2013; Das et al. 2022). In the last decades, Network Science based on mathematical Graph Theory has emerged as a powerful approach for assessing UGS arrangement and functional connectivity (Urban and Keitt 2001; Kong et al. 2010; Hashemi et al. 2024), modeling landscapes as networks of habitat patches (i.e., nodes) linked by potential movement paths (Galpern et al. 2011). Compared to traditional heterogeneity metrics, which are mainly focused on patch geometry rather than mosaic function (Uuemaa et al. 2009; Kupfer 2012), graph-based metrics offer a more functional connectivity analysis (de la Barra et al. 2022).

While some efforts have been made to assess connectivity, these have often been restricted to small areas or specific ecosystems and standardized, cross-city comparative analyses evaluating spatial configurations across diverse international contexts remain scarce. For instance, Villegas et al. (2021, 2024) developed localized frameworks utilizing high-resolution imagery to map morphological spatial patterns, demonstrating that targeted graph-based metrics can effectively reveal habitat fragmentation. Building on these methodological foundations, there is a clear need to scale these structural analyses to broader, cross-national urban networks.

While many studies have explored connectivity at regional or broader spatial scales, this study provides a unique, uniform framework for independently assessing and comparing the structural networks of 28 distinct European capitals. To our knowledge, large-scale studies comparing graph theory with traditional metrics for UGS are lacking, likely due to three main constraints.

First, high-resolution standardized vegetation maps for a relevant number of urban areas are scarce (Yan et al. 2018; Brandt et al. 2023). In this context, remote sensing has witnessed significant advancements in vegetation mapping, primarily due to improvements in temporal, spectral, and spatial resolution of available products (Dash and Ogutu 2016; Wulder et al. 2019; Fraucqueur et al. 2019). In Europe, the Copernicus program (Jutz and Milagro-Pérez 2020) provides Earth observation data from its Sentinel satellites. The Copernicus Land Monitoring Service (CLMS) produces thematic products and in situ data, including nationwide maps of trees and grassland, and urban-specific products like the Urban Atlas (Congedo et al. 2016). Second, processing spatial data over large areas is computationally demanding, though cloud platforms such as Google Earth Engine can mitigate this (Gorelick et al. 2017).

Finally, standardized methods to convert vegetation maps into graphs are limited. Recently, Graphab (Foltête et al. 2012, 2021) has emerged as an operational tool for computing global and local network metrics and has been applied to habitat suitability, planning evaluation, and fragmentation/connectivity studies (Kohler et al. 2016; Duflot et al. 2018; Kim et al. 2019; Kim and Kang 2022; Lumia et al. 2023).

Therefore, the core motivation of this study is to scientifically evaluate the underlying logic of pattern quantification and to demonstrate the limitations of relying solely on simplified abundance metrics. Rather than merely categorizing urban layouts, this research aims to investigate the complex relationships between simple area metrics, traditional landscape ecology metrics, and functional connectivity derived from Graph Theory. By evaluating UGS across 28 European capitals, we explicitly seek to assess whether the percentage of green space adequately represents the spatial configuration and ecological connectivity of urban environments, ultimately providing standardized criteria to guide the selection of appropriate landscape indices for future urban policies.

To do so, we first created an innovative 10 m resolution European Urban Vegetation Map (EUVM) covering 28 European capital cities (EU-28), distinguishing three main vegetation categories: (i) trees, (ii) shrubs, and (iii) grassland. To address computational issues and improve its reproducibility, the process was implemented using the Google Earth Engine (Gorelick et al., 2017) cloud computing platform. After successfully validating the EUVM against field surveys collected through the Land Use and Coverage Area Frame Survey (LUCAS) program, we used the Graphab-based R package "graph4lg" (Savary et al. 2021) to calculate ten graph theory-based metrics also used in Network Science. These metrics were then compared with 30 more traditional landscape metrics - such as landscape aggregation, patch area and edges, core areas, diversity, and patch shape - calculated using the software FRAGSTATS and the related R package "landscapemetrics" (Hesselbarth et al. 2019, 2024). Finally, the results were compared and discussed to assess the relevance of the different metrics in evaluating the spatial arrangement of UGS within the EU-28 capital cities that, through a cluster analysis, were classified according to their (i) city size, (ii) peri-urban forest presence, and (iii) spatial organization of UGS.

2. Materials and methods

2.1. Study area

The study was conducted for the EU-28, including the European Union capital cities and London. The definition of city boundaries is a critical issue, as it directly affects the extent of UGS and related landscape ecology metrics. Here, we used the city boundaries adopted for the 2017 Eurostat Urban Audit data collection, the so-called "Eurobarometer", as they were specifically developed to maximize the comparability of statistics across the very different spatial arrangements of European cities, towns, and Functional Urban Areas (European Commission, 2016). The city boundaries' geographical source - hereinafter referred to as Urban Audit - is available at https://ec.europa.eu/eurostat/web/gisco/geodata/statistical-units/urban-audit (last accessed on 05/22/2025). Next, a 1 km buffer was created around each city to include vegetation patches that could fall across the Urban Audit boundaries, but that are relevant for the ecological network connectivity analysis. Overall, we investigated an area of 11476.55 km^2, covering approximately 0.3% of the total EU-28 area (447,687,200 ha). The cities investigated are very different in size, ranging from 1575 km^2 in London to 39 km^2 in Athens. Overall, the area hosts 52.4 million inhabitants, approximately 10% of the total population in the EU-28 region (Eurostat 2020).

2.2 The European Urban Vegetation Map

The European Urban Vegetation Map (EUVM) was developed at a 10 m spatial resolution for the 2018 reference year, employing a nomenclature system centered on three dominant vegetation types: trees, shrubs, and herbaceous cover. The creation of the EUVM involved integrating five Copernicus Land Monitoring Service products, which were processed and aggregated in the GEE environment to ensure computational efficiency at a continental scale.

The primary framework was provided by the Urban Atlas 2018 (ESA 2018), a vector land-use and land-cover dataset with a Minimum Mapping Unit of 0.25 ha for urban classes and 1 ha for rural classes. To capture vegetation features below these thresholds, supplementary high-resolution layers were incorporated. The Street Tree Layer, a vector product with a Minimum Mapping Unit of 500 m^2, and the 5 m-resolution High Resolution Layer Small Woody Features were used to identify fragmented tree rows and patchy structures. Tree cover was further refined using the High Resolution Layer Tree Cover Density, which was reclassified into a Boolean "trees" layer by applying a 10% minimum density threshold, consistent with FAO forest definitions (FAO 2000). For the herbaceous component, the High Resolution Layer Grassland - a binary dataset derived from integrated Sentinel-1 and Sentinel-2 data - was reclassified as herbaceous vegetation.

To ensure spatial consistency, all vector inputs were rasterized to a 10 m resolution, and all datasets were projected into the ETRS89 Lambert Azimuthal Equal Area coordinate system (EPSG: 3035). These harmonized layers were then reclassified into four final categories (Table 1): (0) non-vegetation, (1) trees, (2) shrubs, and (3) herbaceous vegetation.

Table 1. Reclassification scheme for Copernicus input layers. The codes not included are considered in the EUVM class (0), not vegetation

INPUT – Copernicus layers		**OUTPUT – European Urban Vegetation Map**		
Layer	*Description*	*[1] trees*	*[2] shrubs*	*[3] herbaceous*
Urban Atlas	Land cover classification within European functional urban areas	31000 (Forest)	32000 (Herbaceous vegetation associations) 33000 (Open spaces with little or no vegetation)	21000 (Arable land (annual crops)) 22000 (Permanent crops) 23000 (Pastures) 24000 (Complex and mixed cultivation)
Street Tree Layer	Vector map within European functional urban areas (Artificial surfaces from Urban Atlas)	1	-	-
Tree Cover Density	Percentage map of tree cover density (0-100)	≥10% coverage	-	-
Grassland	Binary map (0 absence of vegetation, 1 grassland)	-	-	1

INPUT – Copernicus layers		**OUTPUT – European Urban Vegetation Map**		
Layer	*Description*	*[1] trees*	*[2] shrubs*	*[3] herbaceous*
Small Woody Features	Binary map (0 absence of vegetation, 1 trees)	1	-	-

The information in the four layers we considered is frequently redundant. For instance, most of the area classified as Small Woody Features has tree cover from the Tree Cover Density above the 10% threshold, though not always. For this reason, in aggregating the layers for the same class, we adopted a conservative approach using the logical operator "OR" (Figure 1).

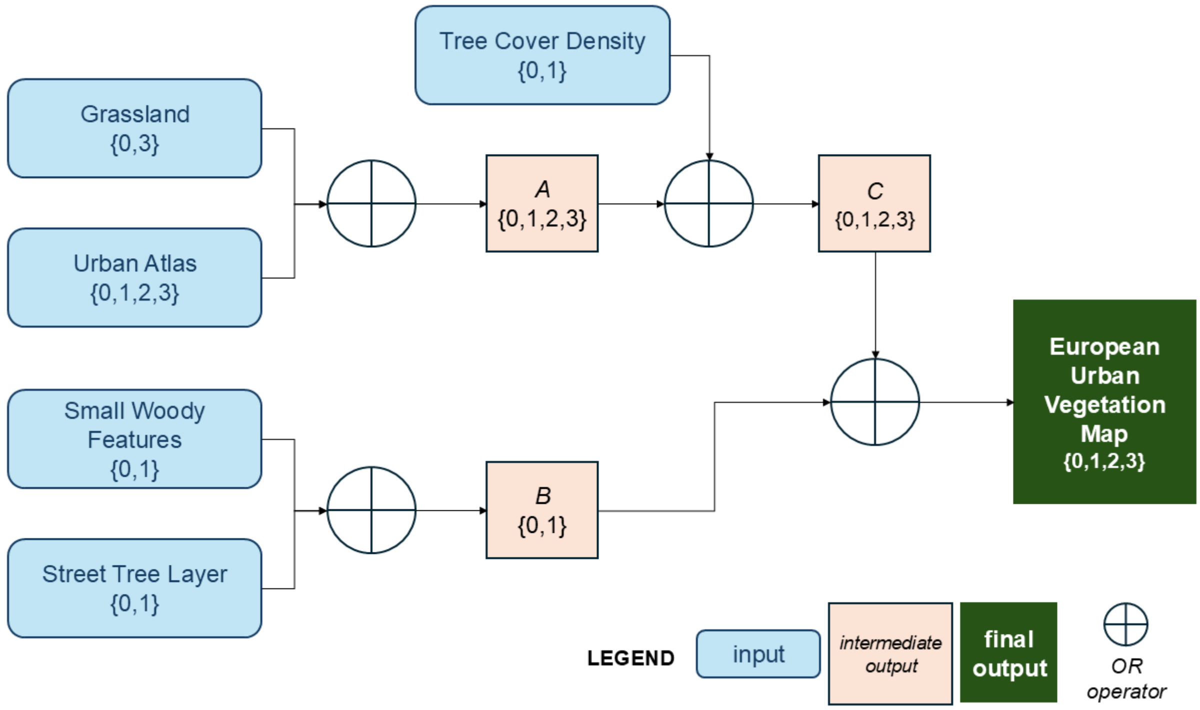

Fig.1 European Urban Vegetation Map flowchart. In the legend {0 for pixels considered as non-vegetated, 1 for tree cover, 2 for shrub cover and 3 for herbaceous cover}.

2.3 Data validation

Before adopting the EUVM for the following analyses, we validated it against information reported in the Land Use and Coverage Area Frame Survey (LUCAS) for the reference year 2018, which is openly available in GEE as a harmonized version of all yearly surveys (d'Andrimont et al. 2020).

To validate the EUVM, we used 337,845 LUCAS second-phase points (Ballin et al. 2018) visited in the field in 2018. Of these, 1866 points fall within the EU-28 city buffers where the EUVM was created. Due to the different definitions used in EUVM and LUCAS, we used a Boolean approach, considering together woodland/shrubland classes from both LUCAS and EUVM.

Based on the 2 x 2 confusion matrix from the LUCAS validation points, we obtained a true positive of 408, true negative of 1154, false positive 84, and false negative 220. Based on this, the resulting overall accuracy of the EUVM was 0.84, producer's accuracy 0.64, and the user's accuracy 0.80. Detailed city-level information is available in the Annex, Table 1A. On the basis of these results, we considered EUVM (Figure 2) as the basis for the following analysis.

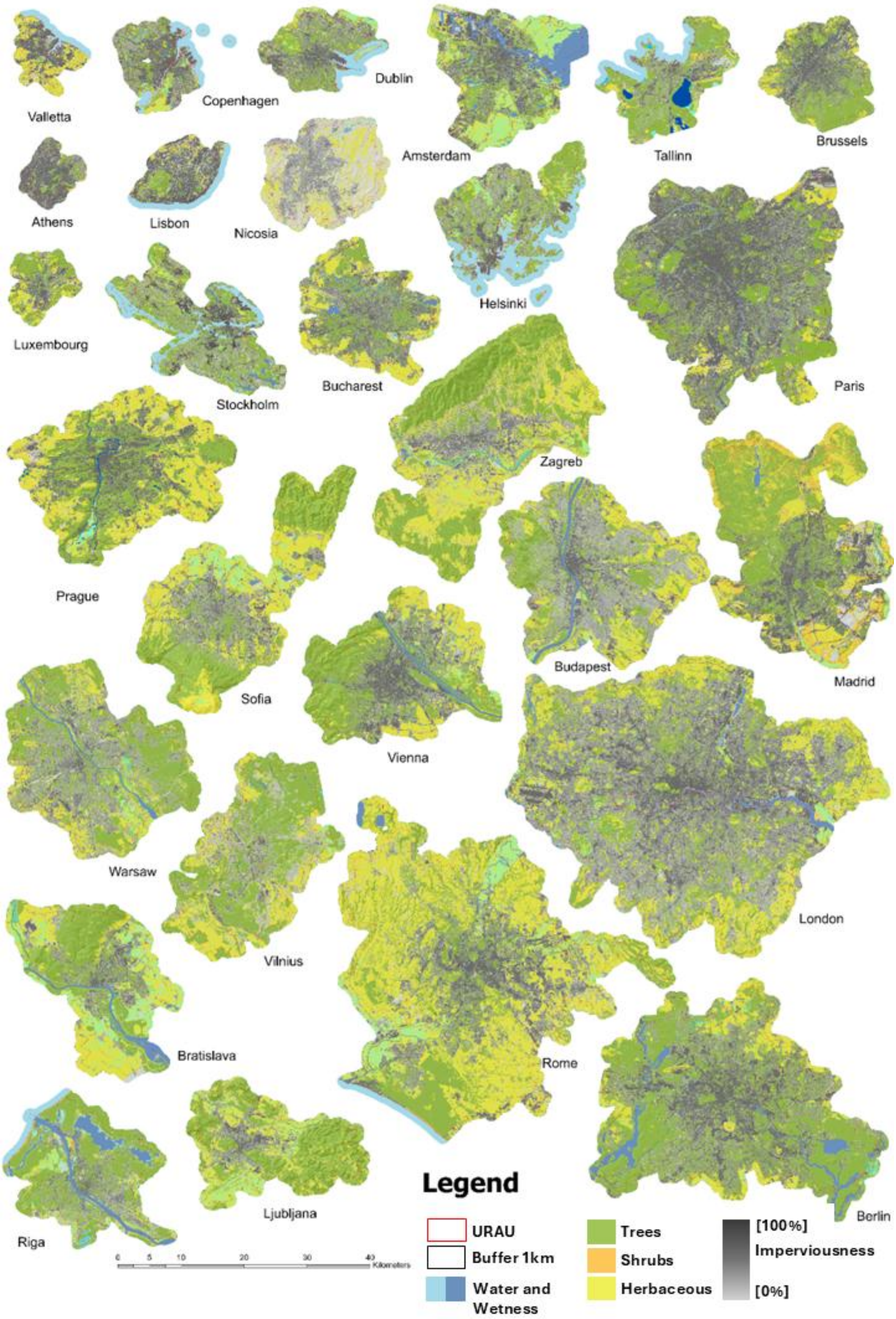

Valletta
Copenhagen
Dublin
Amsterdam
Tallinn
Brussels
Athens
Lisbon
Nicosia
Helsinki
Paris
Luxembourg
Stockholm
Bucharest
Zagreb
Prague
Sofia
Budapest
Madrid
Vienna
Warsaw
Vilnius
London
Bratislava
Rome
Riga
Ljubljana
Berlin
Legend
URAU
Buffer 1km
Water and Wetness
Trees
Shrubs
Herbaceous
[100%]
Imperviousness
[0%]
0 5 10 20 30 40
Kilometers

Fig. 2 The EUVM of the 28 European capitals considered in this study. They are ranked from top left to bottom right based on the cluster analysis available in Figure 8. For a better comprehension of the maps we added to the layouts, the layers of the Copernicus High Resolution Layer for Water and Wetness (in dark and light blues, for permanent inland and sea water, respectively) and for Imperviousness (in gray tones)

2.4 Network connectivity and landscape ecology analysis

For this study, two sets of landscape patterns and network connectivity metrics were computed using two different approaches. FRAGSTAT software (McGarigal et al. 2023) and the related R package “landscapemetrics” (Hesselbarth et al. 2024) were implemented for the calculation of the 30 landscape metrics related to the groups (i) Aggregation (AGG), (ii) Area and Edge (AED), (iii) Core Area (COR), (iv) Diversity (DIV) and (v) Shape (SHP) metrics. Besides, the software Graphab (Foltête et al. 2012, 2021) and the related R package “grap4lg” (Savary et al. 2021) were used for the calculation of the ten Network (NET) metrics. In both cases, the EUVM was used as the input of the analysis, setting the pixels classified as “trees” and “shrubs” as the target habitat categories of the network. The total list of 40 metrics we calculated for each city is reported in the Annex, Table 2A. The approach for the comparison of the indices was inspired by recent review (Uuemaa et al. 2009, 2013).

2.4.1 Network connectivity metrics based on graph theory

For this approach, we used the Graphab metrics (Foltête et al. 2012, 2021) implemented in the R package “graph4lg” (Savary et al. 2021).

First, the EUVM was used to create habitat patches when the cumulative area of adjacent pixels reached at least the minimum patch area threshold of 0.1 hectares (Bulman et al. 2007). Next, from each patch, a node is located in its centroid, and planar links are set between the habitat patches based on the Euclidean distance among them. Here, we consider the matrix as uniform in terms of resistance values of landscape categories. We explicitly acknowledge that assuming a homogeneous resistance surface across the urban matrix is a strong simplification. In reality, varying levels of human activity, built infrastructure, and traffic impose heterogeneous resistance to ecological flows. However, since the primary objective of this study is to compare graph-based network approaches with traditional landscape ecology metrics—rather than to develop highly optimized, localized connectivity models for specific ecological management—a straightforward and unweighted graph analysis was deemed the most appropriate baseline for this methodological comparison.

Lastly, the graph was pruned by setting a maximum distance threshold between patches of 200 m, which previous studies identify as suitable for urban forest landscape connectivity analysis (Chang-Fu et al. 2010).

Based on the graph, we calculated three global metrics that were considered relevant in recent studies on urban landscape connectivity analysis (e.g., Babí Almenar et al. 2019; Mu et al. 2021): (i) the probability of connectivity (PC), (ii) the (relative) equivalent connected area (ECA), and (iii) the integral index of connectivity (IIC).

The PC represents the probability that two individuals, randomly located in the landscape, are situated within interconnected habitat patches (Saura and Pascual-Hortal 2007). It is calculated as the area-weighted probability of connection between all patch pairs and is particularly sensitive to habitat loss. Next, ECA translates the PC value into an equivalent area of a single, maximally connected patch, facilitating interpretation in terms of habitat extent (Saura et al. 2011). To enable comparison across different cities, ECA values are standardized by the total area of each city (Savary et al. 2024). The IIC, in contrast, is based on a binary model of connectivity, reflecting the probability that individuals within a patch can reach each other through existing links. It provides a topological view of the network and increases with greater connectivity (Pascual-Hortal and Saura 2006). While PC relies on probabilistic interactions to capture species-specific movement across the landscape, IIC evaluates structural connectivity based on the presence or absence of links (Bodin and Saura 2010). Both indices range from 0 to 1, with higher values indicating better connectivity.

In addition to these indices, eight additional metrics were used to describe the structure of the habitat network. These include the total, median, and Gini coefficient of patch capacity (area in hectares), the number of links per hectare (including those ≤200 m), their mean and standard deviation in distance, and the Gini index of link distances.

2.4.2 Landscape ecology metrics

For this approach, we used FRAGSTAT metrics (McGarigal and Marks 1995; McGarigal et al. 2023) implemented in the R package "landscapemetrics" (Hesselbarth et al. 2024). Among the vast array of possible metrics, we selected the most relevant based on their use in previous experiences in urban landscapes (Kupfer 2012; Schindler et al. 2015; Chen and Yu 2017; Frazier and Kedron 2017; Das et al. 2020). Overall, we calculated a total of 30 metrics aggregated in five groups: i) aggregation (8), ii) area and edge (9), iii) core area (5), iv) diversity (2), and v) shape metrics (6). See Annex, Table 2A for a short description of the metrics and McGarigal et al. (2023) for a more complete explanation.

2.5. Comparing graph theory and traditional landscape ecology metrics

In this study, we employed a series of statistical analyses to explore the relationships among our metrics and their utility for urban classification and planning.

First, we compared the correlation between the metrics, one against the other, reporting the Spearman's coefficients for each pair. To understand the potential usefulness of the metrics for classifying the different cities according to specific metrics, we repeated the correlation analysis in two ways: first, based on rank scores assigned based on all the metrics (the largest values given the largest ranks), then using averaged metrics based on the six groups reported in Annex, Table 2A, which facilitate the interpretation of their relationships.

Next, to enhance the comprehension of our results and the potential for creating groups of cities with comparable conditions based on the calculated metrics, we performed two multivariate analysis: a hierarchical cluster analysis to formally identify clusters of cities based on the calculated metrics, and a Principal Component Analysis (PCA) of the original dataset, to highlight the relevance of the metrics in differentiating the spatial arrangement of UGS across cities.

Finally, since one of the main goals of this study is to determine if the percentage area covered by UGS (i.e., *AED_pland*) is informative enough for city ranking and urban planning, we used *AED_pland* as a reference value, systematically comparing it with all other indicators through correlation analysis across the cities.

3. Results

In more than half of the urban areas investigated (15 cities out of 28, Figure 3), the UGS share is higher than the European average (52.62%), based on the EUVM. Among those, Ljubljana has the largest share of UGS, covering 78.75% of its territory, mostly with trees (51.80%). On the opposite side, Athens showed the lowest UGS coverage, 19.46% of its territory, followed by Nicosia (25.96%) and Lisbon (26.53%). Following Ljubljana, trees represent the most important UGS category in northern European areas, especially Tallinn and Vilnius (see Annex, Table 3A). In contrast, southern European capitals exhibit a significant proportion of herbaceous cover, notably in Rome, Bratislava, and Zagreb, along with shrubland, predominantly in Madrid and Valletta. Lastly, Mediterranean cities such as Athens recorded the lowest share of UGS among European capitals, with less than 20% vegetation coverage (19.45%). This is followed by Nicosia and Lisbon, each with approximately 26% vegetation coverage.

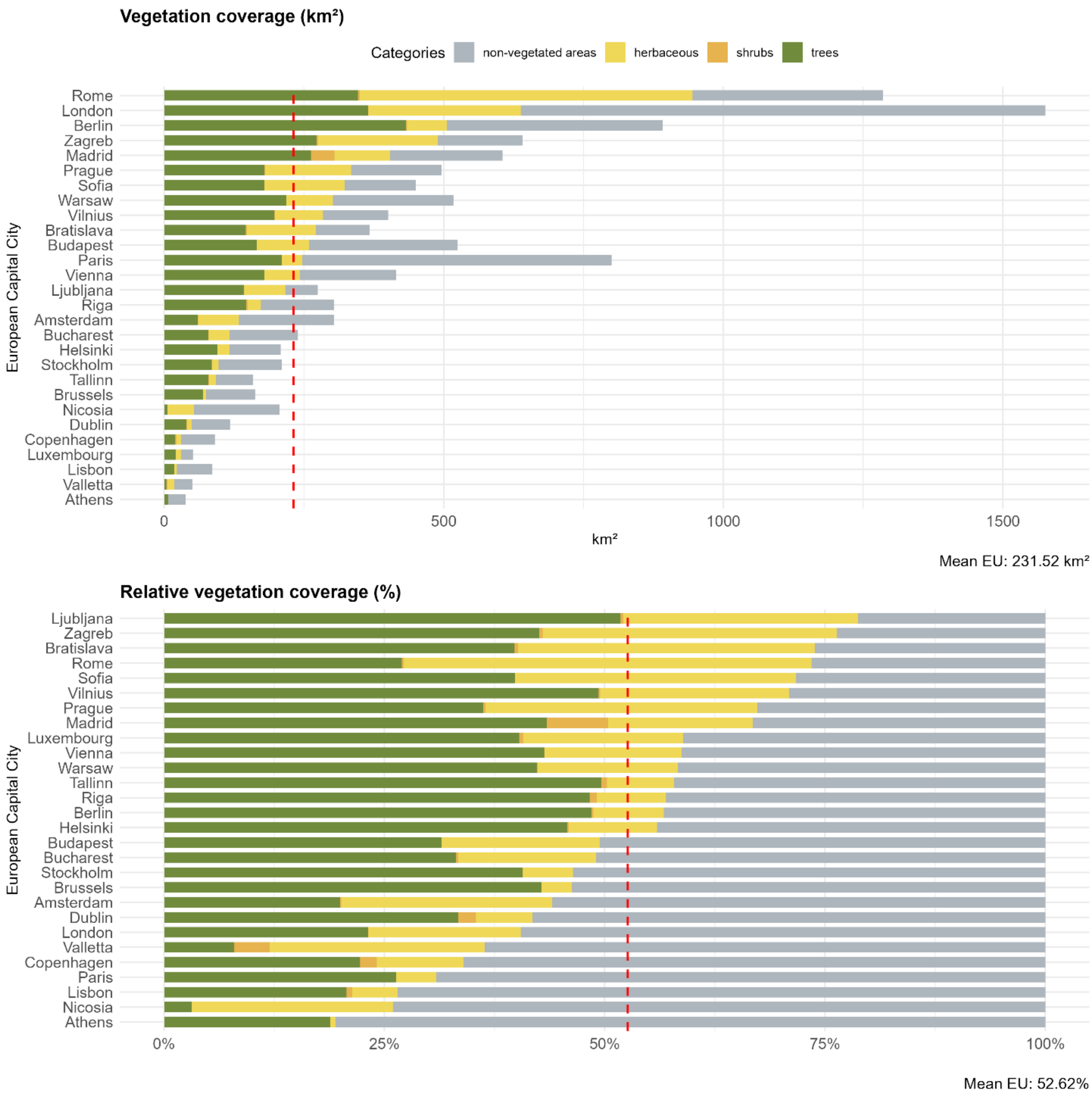

Fig. 3 European capital cities' land cover share in absolute values (above) and as a relative coverage (below) over the total area, according to the European Urban Vegetation Map. Cities are ranked based on the overall share of vegetation over the total area

Based on these results, there is a clear relationship between population density (i.e., number of inhabitants per unit area) and per-capita availability of UGS. So, the higher the population density, the lower (with an exponential law) is the amount of UGS available per capita (Figure 4).

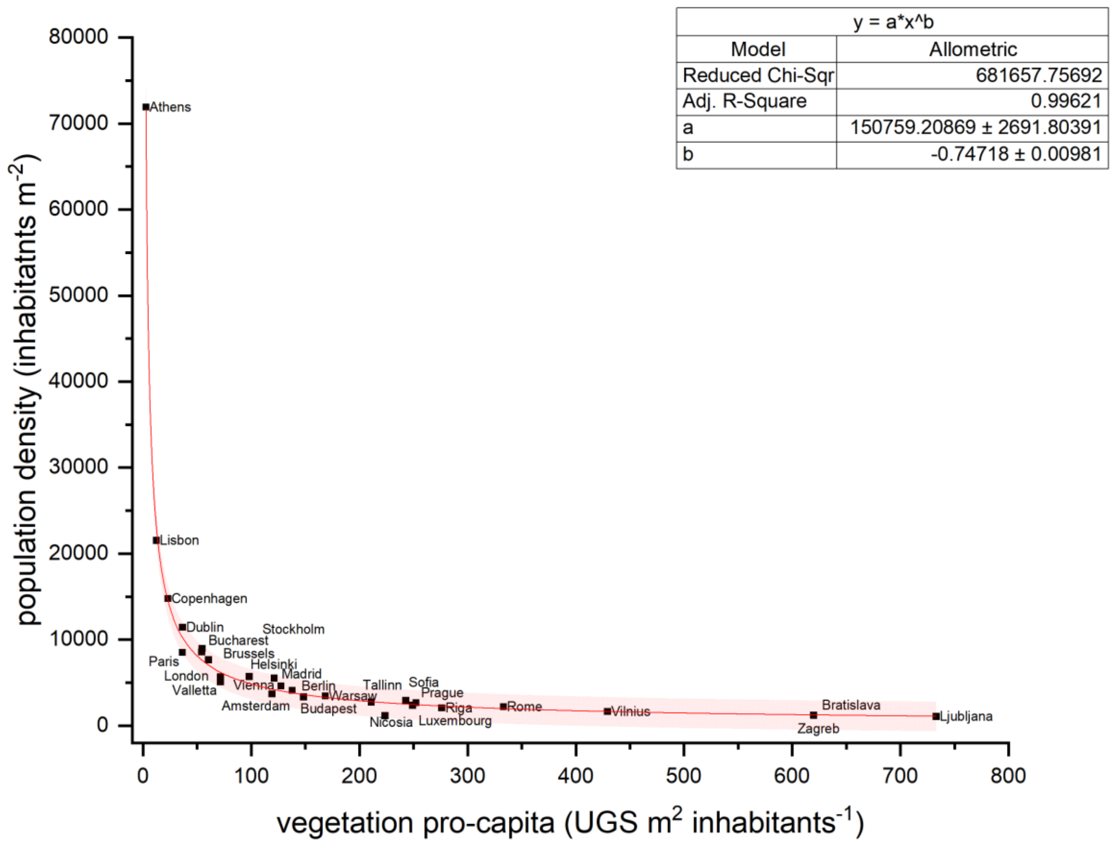

Fig. 4 Population density (inhabitant/km^2) vs. vegetation per capita (m^2/inhabitant) for 28 European capitals. The red curve represents an allometric fit (y=a*x^b) with an adjusted R^2=0.996 and y ≈ 150759 * x$^{-0.75}$).

3.1 Landscape metrics

For each city, the average value of each landscape metric calculated is reported in the Annex, Tables 4-8A, while below we report the details for each group.

3.1.1 Aggregation metrics

Several spatial aggregation metrics (AGG) are related to the percentage amount of UGS available in the different cities, but in general, the average relationship is quite weak (average R^2 = 0.3). We found direct relationships with *AI*, *cohesion*, *enn_CV* or inverse relationships with *division*, *split* (with R^2 up to 0.7). In other cases, the aggregation metrics are not related to the relative amount of UGS in the area and, for this reason, are probably more informative. This is the case of *np* and *LSI* that account respectively for the number of patches and their level of aggregation: a very good example is London where the UGS covers only the 23% of the total area (the 6th lower value within the 28 capitals) but the number of patches (more than 27000) is instead the highest and very disaggregated resulting in the highest value of *LSI*. In general, *np* and *LSI* resulted, as expected, strictly related to each other with a direct linear relationship (R^2 = 0.85).

3.1.2 Area and edge metrics

Within the metrics related to patch area and edge (AED), some theoretical relationships are respected, such as the decreasing exponential relationship between the patch mean area and the number of patches per hectare of UGS (Figure 5).

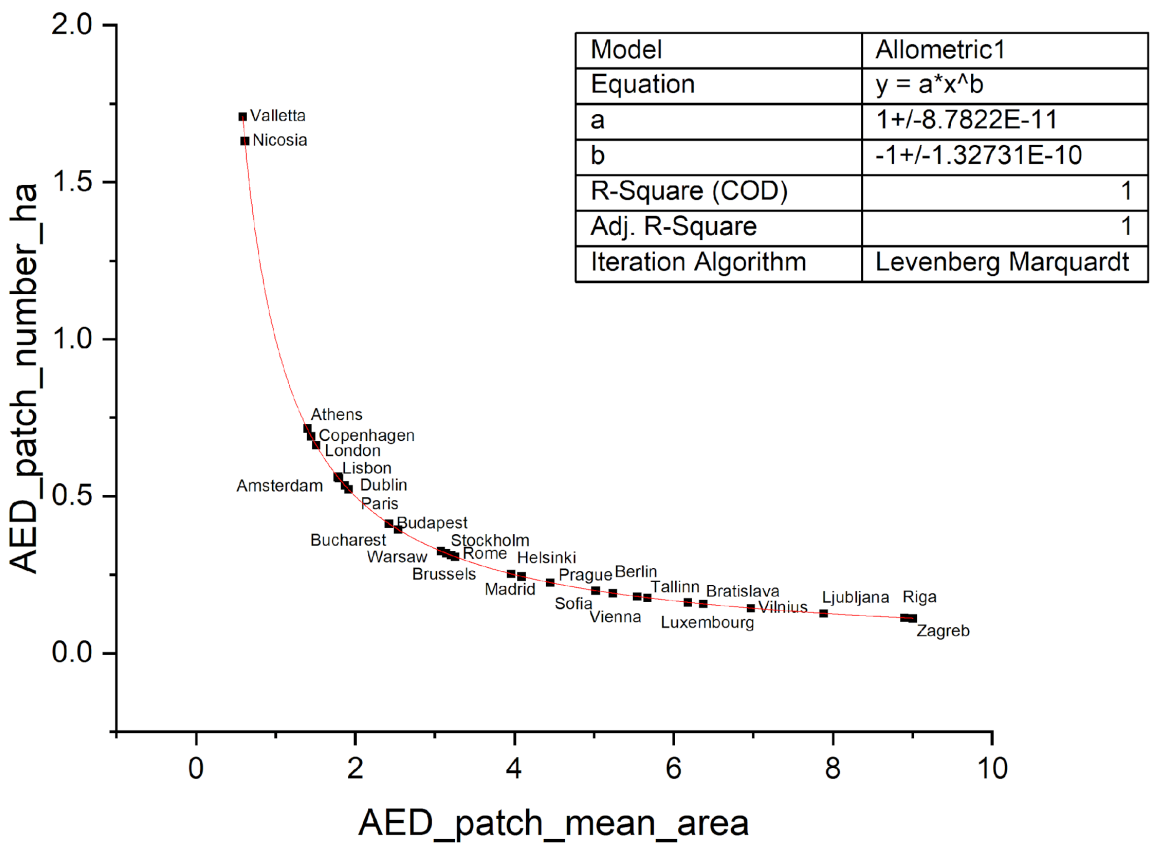

Fig. 5 Patch density (AED_patch_number_ha) versus mean patch area (AED_patch_mean_area) for 28 European capital cities. The data is modeled using an allometric fit ($y=a*x^b$) indicating the distribution of city-specific spatial metrics relative to the fit line.

Based on this relationship, we can easily detect that Nicosia and Valletta account for the lowest average dimension of the patches and the highest density in terms of the number of patches per ha. These cities also account for the lowest percentage of UGS (respectively 3% and 12% of the landscape). Many of the AED metrics are less interesting because linearly directly related to the amount of UGS, such as: *AED_patch_mean_area*, *AED_pland_trees*, *AED_gyrate*, *AED_lpi* (R^2 of 0.63, 0.99, 0.51, 0.46 respectively), or inversely related, like for *AED_patch_number_ha* (R^2 = 0.74).

It is interesting to note that the relationship between UGS total area (*AED_ta*), and its percentage expression against the total landscape areas is quite small (R^2=0.18) because the strong variation in the dimension of the different Capitals makes the comparison between them very difficult.

The only metric not correlated with UGS percentage coverage is the edge density (*AED_ed*), which is instead directly inversely correlated to the aggregation of the patches (inverse linear decreasing relationship with *ADD_pladj*, with R^2=0.99) and sensitive to the shape of the patches too (direct linear increasing relationship with *SHP_para_cv*, with R^2=0.32).

Finally, the metric *AED_pland_shrubs* has limited interest because shrublands represent a very small part of the total UGS area; the average is less than 1% of the investigated areas, with notable exceptions only for Madrid (7%) and Valletta (4%), typical of a more Mediterranean condition.

On average, the correlation between these metrics and the simple indicator of the percentage of area covered by UGS is good (R^2 = 0.42).

3.1.3 Core area metrics

Regarding the core area metrics the empirical analysis of the data confirmed the theoretical direct relationship between the amount of habitat available (*AED_ta*) and the amount of core areas *COR_tca* (R^2=0.98); it is interesting to note, because less theoretical evident, that also the variability in the size of the patches (*AED_area_cv*) is directly correlated to the variability in the size of the core areas (*COR_core_cv*) with R^2=0.99. The relationship between the percentage of the core areas on the total UGS (on the y axis) and the percentage of UGS on the total investigated areas (on the x axis, Figure 6) can easily represent the situation with Capitals poor in percentage coverage of the UGS that are also poor in core areas (R^2 = 0.66) such as Nicosia and Valletta. The percentage of core areas is directly correlated with the average dimension of the patches (R^2 = 0.73).

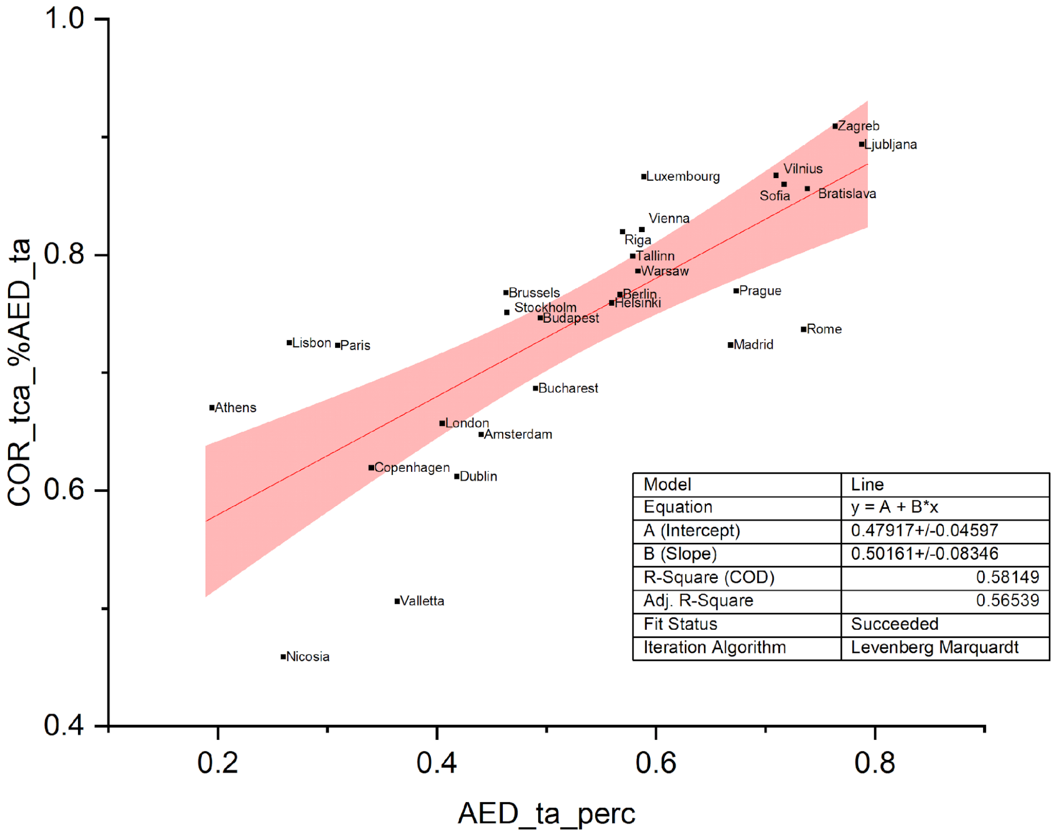

Fig. 6 Correlation between the percentage of the core areas on the total UGS (COR_tca_%AED_ta) and the percentage of UGS on the total investigated areas (AED_ta_perc). Each data point represents an individual European capital, showing their distribution relative to the linear trend line.

Here, the number of disjunct core areas (*COR_dcad*) is inversely related to the presence in the landscape of very large patches (*AED_lpi*, R^2 = 0.41) but once again directly related to the percentage of UGS (R^2=0.61). On average, the correlation between these metrics and the reference indicator percentage of area covered by UGS is weak (R^2=0.27).

3.1.4 Diversity metrics

The diversity metrics exhibited moderate collinearity (R^2 = 0.42). This relationship is likely constrained by the thematic detail available in the EUVM, which only classified UGS into three broad classes: trees, shrubs, and herbaceous coverage. For a more meaningful diversity analysis, at least the main tree species or categories should be mapped. Nevertheless, the average correlation between these metrics and the reference indicator percentage of area covered by UGS is very poor (R^2=0.29), while both of them are very much related with an inverse exponential rule to the UGS area expressed as a total (R^2=0.95 for *DIV_prd* and 0.46 with *DIV_sidi*). The relationship between the total area covered by UGS and *DIV_prd* is available in the Annex, Figure 10.

3.1.5 Shape metrics

The shape metrics demonstrate, as expected, good independence from the amount of UGS in the landscape, regardless of whether analyzed in absolute or relative terms. Only the variability in the patch shapes (i.e., *SHP_frac_cv*, *SHP_para_cv*, *SHP_shape_cv*) demonstrates a (weak) direct relationship with the percentage amount of UGS in the landscape (R^2 of 0.22, 0.24, and 0.34, respectively). Indeed, the three types of metrics we used for accounting the patch shape complexity are linearly correlated among each other, but while the fractal dimension (*SHP_frac_mn*) has good agreement both with the perimeter/area ratio (*SHP_para_mn*) and with the shape index (*SHP_shape_mn*) (R^2 of 0.71 and 0.79 respectively) the perimeter/area ratio has only limited agreement with the shape index (R^2 = 0.3).

The variability of the three metrics demonstrates good agreement within them and direct weak agreement with the average dimension of the patches (R^2 of 0.18 between *AED_ta* and *SHP_shape_cv*) and with the dimension of the largest patch (R^2 of 0.14 between *AED_lpi* and *SHP_para_cv*).

The average correlation between these metrics and the reference indicator percentage of area covered by UGS is very weak (R^2=0.17).

3.1.6 Network metrics

An example of the ecological network reconstructed with graph theory analysis using Graphab is available in Figure 7 for the city of Paris. Information for all the EU Capital cities is available in the Annex, Figure 11. Regarding the three main NET metrics calculated with Graphab, it is important to note that they are very redundant (with positive linear relationships with R^2 ranging between a minimum of 0.76 and a maximum of 0.97). When the analysis is repeated in the rank order of the cities, the results are almost identical, regardless of the metrics used. The second information is that the relationship between these three metrics and the reference metrics *AED_pland* ranges between 0.45 and 0.57 (and between 0.62 and 0.66, when repeated based on the rank).

Some interesting relationships were also found comparing graph-theory-based metrics and the other landscape metrics calculated with FRAGSTATS. The three NET metrics are directly correlated with the mean dimension of patches (*AED_patch_mean_area*) with R^2 around 0.6 and inversely with *AGG_division*, also approximately with R^2=0.6 and a direct one with *AED_lpi* and with *COR_core_cv* (R^2 of 0.59 and 0.34, respectively).

The amount of links of the networks created in Graphab (*NET_links_mean_lenght*) is directly and strictly related to the number of patches in the area (*AED_patch_number_ha*) with R^2 of 0.87, and inversely with the relative coverage of the vegetated area (*AED_pland*) with R^2 of 0.68; but their average length is not related to the average size of the patches but has just a limited direct relationship with the number of patches in the area (R^2 of 0.24) and an inverse relationship with the relative coverage of the vegetated area (R^2 of 0.44). The variability in the length of the links (*NET_links_sd_lenght*) is not related to the variability in the dimension of the patches but is very much directly related only to the average length of the links (R^2 of 0.68).

The Gini indicator when calculated on the patch capacity is quite redundant with the more traditional indexes related to patch density and size (inverse relationship with the density of the patches expressed by *AED_patch_number_ha* with R^2 of 0.93 and direct relationship with the size of the patches expressed by *AED_patch_mean_area* with R^2 of 0.68 and with relative coverage of the vegetated area expressed by *AED_pland* with R^2 of 0.8.

While when the Gini indicator is calculated on the patch distance expressed by the links length it is very weakly related the size and shape of the patches, for example R^2 of 0.25 with the relative coverage of the vegetated area expressed by *AED_pland* or R^2 of 0.49 with the variability in the fractal dimension of the patches expressed by *SHP_frac_cv* but only very weakly with their average dimension (R^2 of 0.18 with *AED_patch_mean_area*).

Finally, the last two metrics based on patch capacity (*NET_tot_patch_capacity* and *NET_Patch_mean_capacity*) are redundant with the total habitat area (*AED_ta*) and the average size of the patches (*AED_patch_mean_area*), respectively. This may be because, in this study, the capacity of each node in the network generated with Graphab is determined by the size of the patch.

Overall, the correlation among the different metrics is available in the Annex (Figure 12) and the average correlation between these metrics and the reference indicator percentage of UGS is in the average (R^2=0.45).

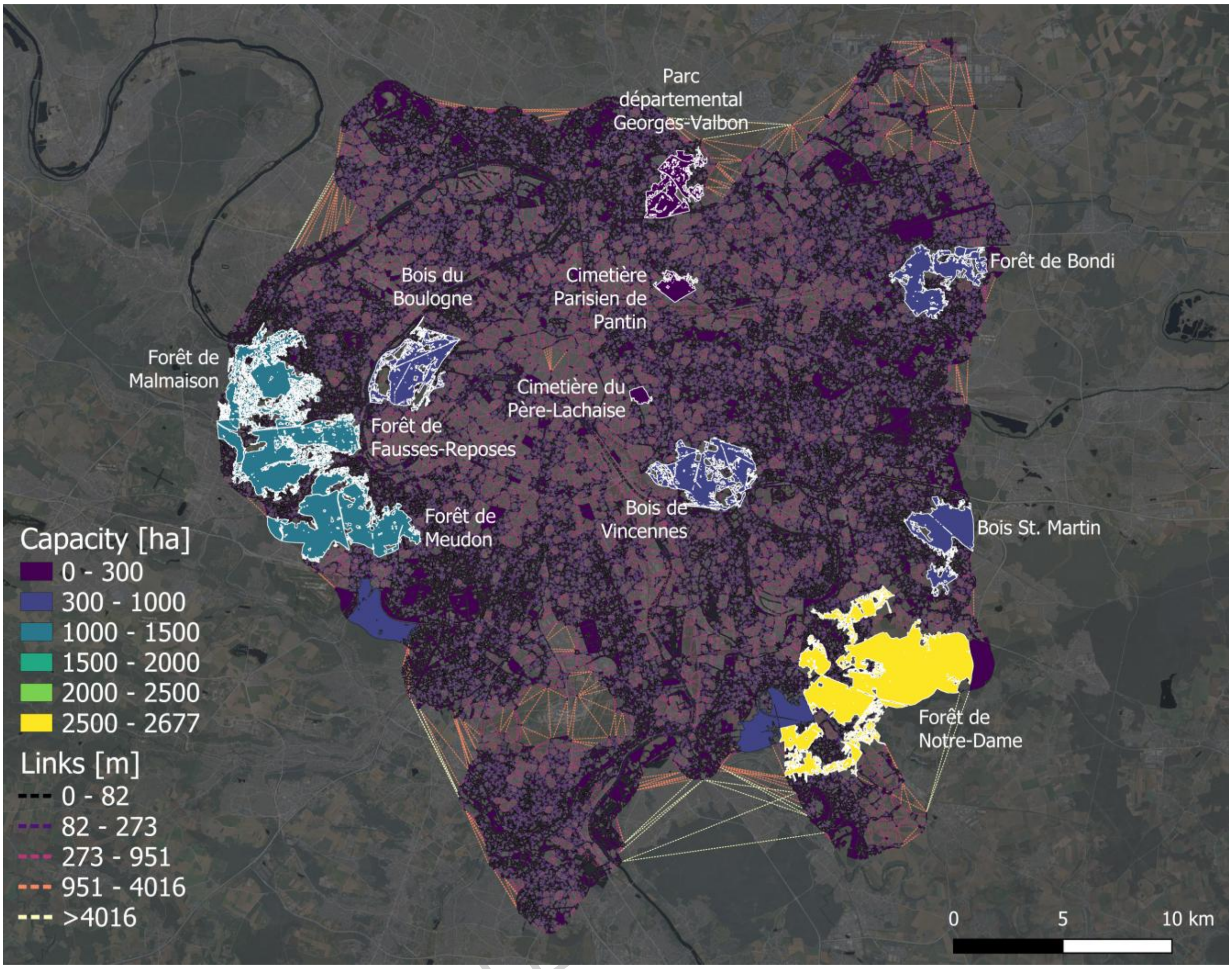

Fig. 7 Network connectivity of Urban Green Spaces (UGS) in the Paris area derived from Graphab analysis. The map illustrates the spatial distribution of patches, categorized by their capacity (ha), and the connectivity links (in m) between them. Major ecological nodes are identified by their local toponyms (in white) to contextualize the network structure.

3.2 Cluster analysis and ranking

The result of the cluster analysis (Figure 8), together with those from the PCA (Figure 9), can improve the comprehension of the similarities between the analyzed cities and the role of the metrics we used for the description of UGS spatial arrangement.

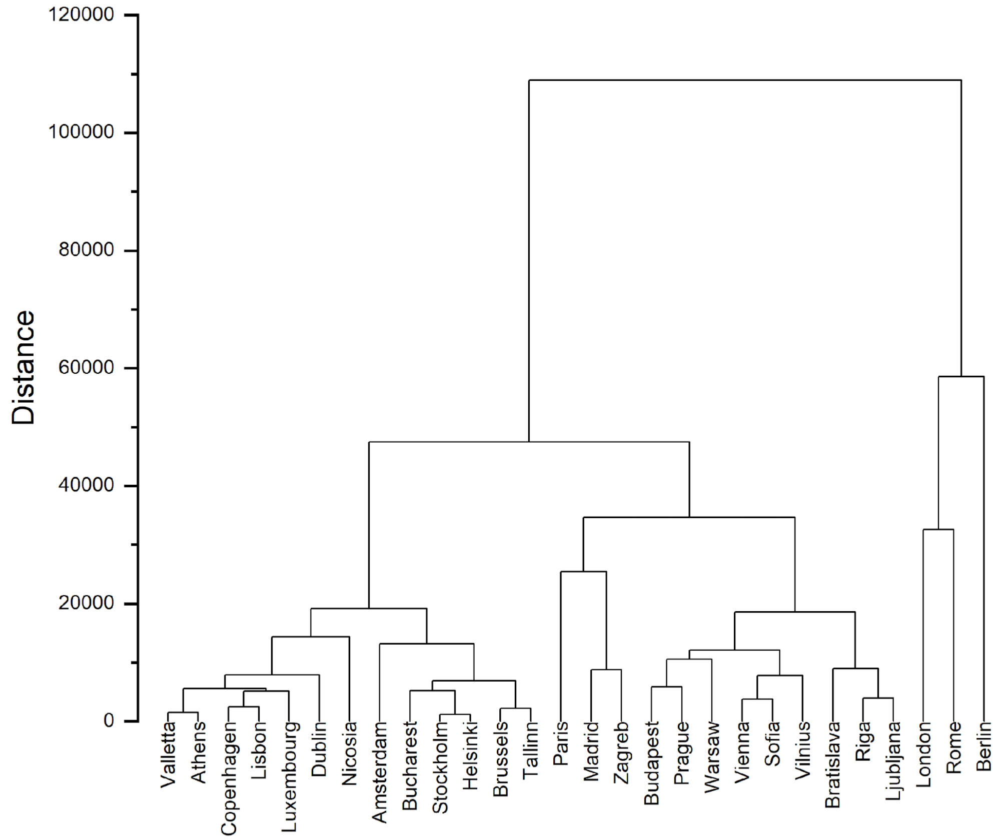

Fig. 8 Dendrogram of hierarchical cluster analysis for European cities based on urban green space (UGS) metrics. The vertical axis indicates the linkage distance between clusters. Cities are grouped according to similarities in their spatial arrangement and dimensions of green areas, identifying distinct clusters from smaller, less connected systems (left) to larger and more connected ones (right)

In Figure 8, there is an interesting ranking of the cities from left to right that can be interpreted as the effect of both the areas' dimensions and the spatial arrangement of UGS. Valletta and Athens are, in fact, relatively small cities, with limited UGS and weak connections in their ecological networks. Another group of relatively small cities, with broader availability of UGS than the previous group, comprises Copenhagen, Lisbon, Nicosia, Dublin, and Luxembourg. This is also confirmed by the PCA, with all these cities showing lower values on the first principal component (Figure 9).

On the right side of the dendrogram (Figure 8), we can find the largest cities (i.e., Berlin, Rome, and London). The city of Berlin has large urban forest areas distributed around the city center (the PCA indicates this pattern is similar to that of Sofia). Moving to the left in the dendrogram we can find those cities that emerged as those with a more relevant connectivity of UGS (Ljubljana, Riga and Bratislava and then in a second cluster with Vilnius, Sofia and Vienna and a third one with Warsaw, Prague and Budapest), these cities have a smaller dimension but with a very consistent and highly connected system of relatively large forest areas in the peri-urban areas as well as green areas in the inner urban area.

The remaining cities exhibit more intermediate characteristics, both in terms of size and the connectivity of UGS, with fewer extensive forested areas adjacent to urban zones. Based on the results of the cluster analysis, specifically the sum of distances within clusters, Bratislava emerges as the most representative city, while London is the least representative.

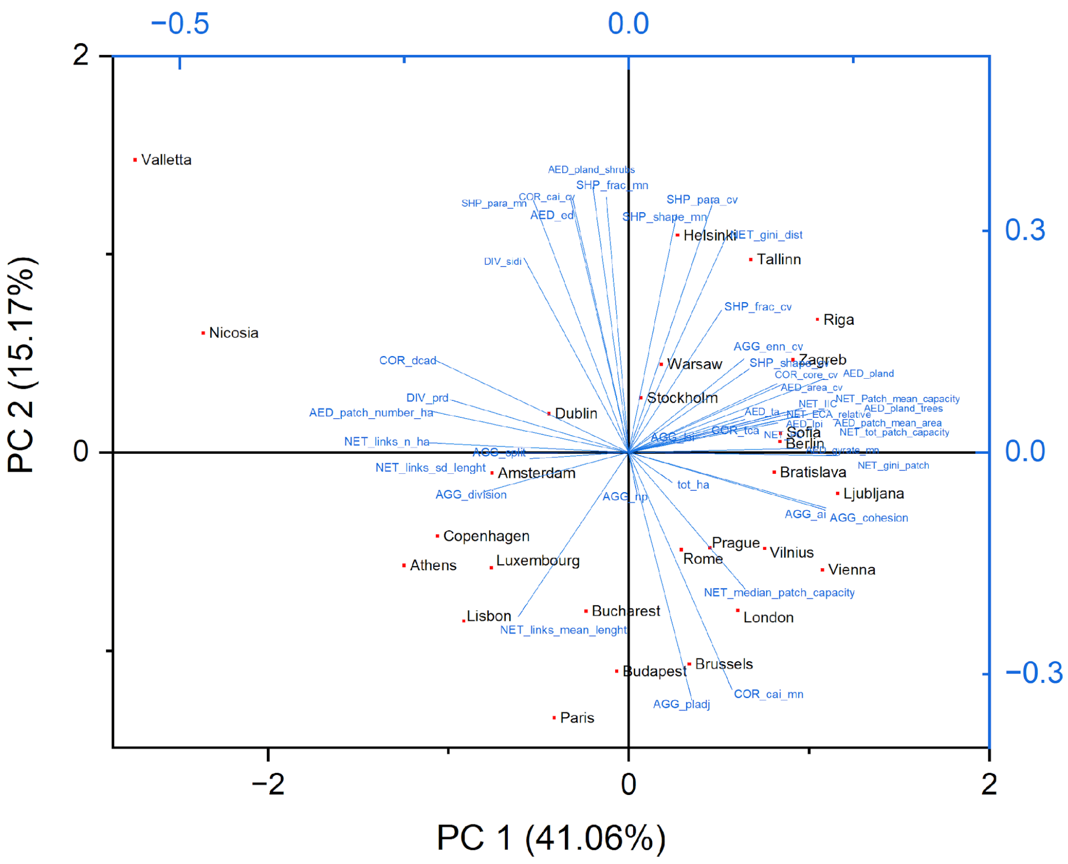

Fig. 9 Representation of the PCA results with eigenvectors and eigenvalues for the different metrics and the position of the 28 cities in the bidimensional space created with the first two components

4. Discussion

4.1. The impact of city boundary definition on comparative analysis

The first information to be considered for discussing the results we achieved is the role of the very different sizes of the cities we analyzed. They range between very large landscapes such as London and Rome (respectively 1575 and 1286 km^2) or Berlin and Paris (respectively 892 and 800 km^2) to very small cities such as Luxembourg, Valletta, or Athens (52, 50, and 39 km^2 respectively). Such variability is in part due to real differences in built-up areas and in part to the different approaches used to define the boundaries of urban areas in the European Urban Audit dataset. The impact of such differences on the assessment of UGS is well known (Raciti et al. 2012). Indeed, at the political level, the attempt to develop a standardized methodology for defining the boundaries of cities has already been documented (Dijkstra et al. 2019), recently leading to a new proposal based on population gridded spatial information (Eurostat 2021). While awaiting a new official, revised version of the boundaries of these European urban areas, the results we achieved can be used to assess the relationships among the different metrics, but not, in our opinion, to produce a conclusive ranking of the cities based on the different spatial arrangements of UGS. Nevertheless, based on the cluster analysis results, we identified three main groups of cities. A first group of relatively small cities with poor availability of UGS and limited ecological connectivity where the limited size also limit the possibility to have in the UGS large forest peri-urban areas, followed by a group of medium-size cities with strong differences in terms of spatial arrangement of UGS but with a consistent component of peri-urban forest area and finally a small group of very large cities where the size of the urban areas determine very different conditions with a complex landscape mosaic and a vast interconnected system of UGS.

4.2. Interrelationships among landscape metrics and urban classification

Given the necessary precautions regarding the impact of city dimension on the metrics, our analysis focused on identifying and interpreting the relationships among the various landscape metrics.

In detail, one of the founding motivations for this study is to assess the relationship between the reference indicators most frequently used to assess and rank cities' green infrastructure, the percentage of area covered by UGS (as also recently introduced by the EU Regulation 2024/1991 on nature restoration), and other metrics related to their spatial arrangement.

Our empirical results confirmed the relationships between landscape metrics that we already know from their theoretical definition (Forman 1995). In fact, in our dataset, when the area covered by UGS constitutes a larger percentage of the landscape, patch density is lower and average patch size is higher (i.e., a few large patches), and thus the relative amount of core areas is also higher. Overall, the agreement between the percentage of area covered by UGS and other indicators was weak (R^2=0.34), especially for patch shape (0.17), core areas (0.27), diversity (0.29), and aggregation (0.30). Indicators for area, edges, and graph theory showed higher correlations (0.42 and 0.45). This examination was particularly significant due to the inclusion of several graph theory metrics. Our results show that these three metrics, namely the Equivalent Connected Area, the Integral Index of Connectivity, and the Probability of Connectivity, are highly redundant, especially when analyzed using rank order. When ranking cities based on the last two metrics, 12 cities share the same rank, and only 13 have a difference of just one position. In contrast, the ranking comparison between the relative Equivalent Connected Area and the other two metrics shows consistent changes: Tallinn shifts by 8 positions, Stockholm by 5, Bratislava by 4, five cities by 3, another five by 2, seven by 1, and seven show no change.

In order to better understand the meaning of these three graph theory metrics, it is important to understand their relationship with the amount of UGS in the different cities. For example, Tallinn has a relatively small part of its landscape covered by UGS, but the patches are well connected, the same, even if with a lower magnitude in

Stockholm. This means that when the cities are ranked on the basis of graph-theory metrics, they may result in different ranking positions despite recording similar values in traditional landscape metrics, and vice versa. However, as recommended by Saura and Pascual-Hortal (2007), the intrinsic characteristics of these metrics should be carefully considered. For instance, the Integral Index of Connectivity assigns higher values to patches at short and intermediate distances compared to Probability of Connectivity, impacting the overall connectivity assessment (Bodin and Saura 2010). Moreover, the potential discrepancies between probabilistic (the latter) and binary (the former) connectivity metrics arise from their inherent characteristics. Despite the strong positive correlation between them, current research suggests that, when confronted with conflicting results, urban landscape management should prioritize probabilistic metrics, as this appears to be a more suitable approach and helps prevent oversimplification of patch connections (Babí Almenar et al. 2019).

4.3 Opportunities and limitations

This analysis focused specifically on the 28 European capitals and presents several key opportunities for urban ecological planning by demonstrating that graph-theory-based metrics, when combined with traditional landscape ecology metrics, offer a more comprehensive assessment of UGS spatial arrangement and connectivity than relying solely on the oversimplified percentage area covered by UGS. This multi-metric approach challenges the utility of the percentage of the total landscape that belongs to a class (e.g., trees or shrubs) as a standalone policy indicator, given its poor correlation with most spatial metrics, and provides a standardized, scalable methodology using Earth observation data for cross-city comparisons. The cluster analysis further provides an opportunity for developing context-specific planning strategies by grouping cities based on size and UGS arrangement.

However, a continuous continental analysis remains currently unfeasible, as the availability of essential high-resolution datasets – such as the Urban Atlas and the Street Tree Layer - is restricted to specific European urban functional zones rather than the entire landmass. Similarly, the present analysis is constrained by the high heterogeneity in urban boundary definitions and varying data coverage, which precludes establishing a conclusive city-rank analysis. Indeed, reliance on specific urban forms and administrative boundaries may introduce bias, since characterizing urban form is highly sensitive to the spatial extent of the analysis (Schwarz 2010). These perimeters may not fully capture functional ecological connectivity in polycentric urban systems compared with monocentric ones, and may thereby overestimate fragmentation in the former. Furthermore, the low thematic resolution of the EUVM, which classifies UGS into only three broad classes, limits the effectiveness of diversity metrics and suggests that future mapping should include the main tree species or additional categories to enable a more meaningful ecological assessment. Indeed, challenges remain in systematically mapping small-scale green spaces (e.g., single tree species, especially in private gardens), non-tree species, and understory vegetation in urban environments (Amir Reza Shahtah massebi 2018; Neyns and Canters 2022).

Furthermore, any comprehensive landscape analysis must address scale dependence (Wu 2004). Landscape metrics and connectivity indices are inherently sensitive to both the spatial resolution and the extent of the study area (Uuemaa et al. 2013). In this study, our assessment was strictly constrained to a 10-m resolution. This specific resolution was dictated by the need to maintain consistency across the 28 European capitals, given the standardized input layers available. While higher resolution does not automatically imply greater suitability for all ecological targets, future studies should consider multi-scale analyses to better capture the nested hierarchies of urban ecosystems. Additionally, future localized applications of our framework should replace our homogeneous baseline matrix with heterogeneous resistance surfaces that reflect the true friction imposed by varying intensities of human urban activity. Although our methodological approach evaluates general structural connectivity, its practical relevance becomes fully apparent when linked to the ecological requirements of indicator or umbrella species. Identifying umbrella species is a well-recognized strategy for urban biodiversity conservation, as securing their habitat networks simultaneously protects numerous co-occurring species (Sattler et al. 2013; Choi et al. 2023). For instance, species sensitive to habitat fragmentation—such as certain avian species or small urban mammals—require specific core area sizes and maximum dispersal distances. The graph-based indices and traditional metrics computed in our framework (e.g., inter-patch distances, functional links, and core area extent) provide the exact quantitative variables needed by urban planners to model habitat suitability and structural corridors tailored to the movement capacities of these critical umbrella species.

Finally, it is important to acknowledge that the current assessment relies heavily on the two-dimensional "percentage of UGS", which represents a horizontal characterization of urban vegetation. A critical future direction for urban ecology is the shift from 2D distribution to 3D structural assessment. In recent years, LiDAR technology has been widely adopted to monitor the three-dimensional structure and carbon stocks of urban forestry (Dong et al. 2025a). While some large-scale canopy height models have been developed, their performance in complex urban environments often remains insufficient to fully and accurately characterize urban trees without the aid of high-precision airborne LiDAR (Dong et al. 2025b). Future implementations of our framework should aim to integrate these 3D metrics to better capture the vertical complexity and true volumetric ecosystem services of urban green spaces.

5. Conclusions

Based on this research, we can draw four main conclusions. First, remote sensing, particularly Copernicus products, provides a robust basis for standardized mapping of urban vegetation in Europe. Using Copernicus layers, we produced a 10 m European Urban Vegetation Map with an overall accuracy of 0.84, adequate for analyzing UGS spatial configuration in major European cities. We recommend extending the EUVM to all European cities in the future and updating it as new Copernicus products become available. The recent release of Copernicus High Resolution Layers (e.g., Cropland) will improve discrimination between herbaceous vegetation and agricultural land by incorporating land-use information. Also, future studies should consider mapping dominant urban tree species to obtain a more refined biodiversity assessment.

Second, the commonly used indicator “percentage of UGS” is overly simplistic for ranking or monitoring urban greening. It should be reported alongside metrics that capture patch shape, core-area extent, spatial arrangement, and compositional diversity. Although these limitations are well known in landscape ecology, this study provides the first quantitative, across-capital evidence that reliance on percent-cover alone can be misleading; we therefore encourage reconsideration of its primacy in official guidance such as the newly adopted EU Regulation 2024/1991 on nature restoration. While the targets set by Article 8 concerning the share of urban green space are essential baseline measures, our results strongly suggest that such indicators are ecologically risky if used in isolation to assess urban ecosystem resilience.

Third, graph-based connectivity analysis is a valuable complement to traditional landscape metrics, revealing aspects of UGS spatial organization not captured by conventional tools and identifying candidate areas for targeted planting or planning to enhance connectivity. Graphab and the graph4lg R package allow the computation of local metrics for each habitat patch and the spatial interpolation of results. However, graph metrics should be interpreted alongside standard landscape indicators: some cities with clearly different UGS configurations can exhibit similar network metric values, underscoring the need for a combined approach.

The classification of cities derived from our analysis serves not as a mere typological exercise, but as clear evidence that simple area metrics fail to capture the complex, multi-dimensional nature of urban ecological networks. Establishing these standardized, multi-metric criteria is imperative to ensure that future urban greening efforts enhance ecological functionality rather than merely increase disconnected green areas across all European capitals. The resulting dataset can support stakeholders and policymakers by improving visualization and comparative analysis, informing interventions to promote sustainable, biodiverse, and socially inclusive urban green infrastructure.

Finally, while this study confirms that the percentage of green space is an inadequate proxy for functional connectivity, more theoretical analysis should be conducted in future research. Developing advanced network models that integrate multi-scale dynamics, heterogeneous resistance surfaces, and the specific requirements of umbrella species will be the next critical step in bridging the gap between theoretical landscape ecology and applied urban planning.

6. References

Afrifa JK, Monney KA, Deikumah JP (2022) Effects of urban land-use types on avifauna assemblage in a rapidly developing urban settlement in Ghana. Urban Ecosyst. https://doi.org/10.1007/s11252-022-01281-0

Amir Reza Shahtah massebi (2018) Remote sensing of urban green spaces: A review | Elsevier Enhanced Reader. 1–37

Babí Almenar J, Bolowich A, Elliot T, et al (2019) Assessing habitat loss, fragmentation and ecological connectivity in Luxembourg to support spatial planning. Landsc Urban Plan 189:335–351. https://doi.org/10.1016/j.landurbplan.2019.05.004

Ballin M, Barcaroli G, Masselli M, Scarnó M (2018) Redesign sample for Land Use/Cover Area frame Survey (LUCAS) 2018

Bodin Ö, Saura S (2010) Ranking individual habitat patches as connectivity providers: Integrating network analysis and patch removal experiments. Ecol Modell 221:2393–2405. https://doi.org/10.1016/j.ecolmodel.2010.06.017

Brandt J, Ertel J, Spore J, Stolle F (2023) Wall-to-wall mapping of tree extent in the tropics with Sentinel-1 and Sentinel-2. Remote Sens Environ 292:113574. https://doi.org/10.1016/j.rse.2023.113574

Bulman CR, Wilson RJ, Holt AR, et al (2007) MINIMUM VIABLE METAPOPULATION SIZE, EXTINCTION DEBT, AND THE CONSERVATION OF A DECLINING SPECIES. Ecol Appl 17:1460–1473. https://doi.org/10.1890/06-1032.1

Chang-Fu L, Bin Z, Xing-Yuan H, Wei C (2010) Selection of distance thresholds of urban forest landscape connectivity in Shenyang City. Yingyong Shengtai Xuebao 21:

Chen Y, Yu S (2017) Impacts of urban landscape patterns on urban thermal variations in Guangzhou, China. Int J Appl Earth Obs Geoinf 54:65–71. https://doi.org/10.1016/j.jag.2016.09.007

Choi J, Park C, Kim S, et al (2023) Habitat probability prediction of umbrella species in urban ecosystems including habitat suitability of prey species. Landsc Ecol Eng 19:417–431. https://doi.org/10.1007/s11355-023-00550-0

Clauzel C, Jeliazkov A, Mimet A (2018) Coupling a landscape-based approach and graph theory to maximize multispecific connectivity in bird communities. Landsc Urban Plan 179:1–16. https://doi.org/10.1016/j.landurbplan.2018.07.002

Congedo L, Sallustio L, Munafò M, et al (2016) Copernicus high-resolution layers for land cover classification in Italy. J Maps 12:1195–1205. https://doi.org/10.1080/17445647.2016.1145151

d'Andrimont R, Yordanov M, Martinez-Sanchez L, et al (2020) Harmonised LUCAS in-situ land cover and use database for field surveys from 2006 to 2018 in the European Union. Sci Data 7:352. https://doi.org/10.1038/s41597-020-00675-z

Das DN, Chakraborti S, Saha G, et al (2020) Analysing the dynamic relationship of land surface temperature and landuse pattern: A city level analysis of two climatic regions in India. City Environ Interact 8:100046. https://doi.org/10.1016/j.cacint.2020.100046

Das S, Kumar Shit P, Bera B, Adhikary PP (2022) Effect of urbanization on the dynamics of ecosystem services: An analysis for decision making in Kolkata urban agglomeration. Urban Ecosyst 25:1541–1559. https://doi.org/10.1007/s11252-022-01246-3

Dash J, Ogutu BO (2016) Recent advances in space-borne optical remote sensing systems for monitoring global terrestrial ecosystems. Prog Phys Geogr Earth Environ 40:322–351. https://doi.org/10.1177/0309133316639403

de la Barra F, Alignier A, Reyes-Paecke S, et al (2022) Selecting Graph Metrics with Ecological Significance for Deepening Landscape Characterization: Review and Applications. Land 11:338. https://doi.org/10.3390/land11030338

Dijkstra L, Poelman H, Veneri P (2019) The EU-OECD definition of a functional urban area. OECD Reg Dev Work Pap Éditions OCDE. https://doi.org/doi.org/10.1787/d58cb34d-en

Dong H, Tang L, Liu J, et al (2025a) Remote sensing of urban tree carbon stocks : A methodological review. ISPRS J Photogramm Remote Sens 227:570–593. https://doi.org/10.1016/j.isprsjprs.2025.06.030

Dong H, Xu Z, Wu J, et al (2025b) High-precision airborne LiDAR remains essential for urban forestry : Revealing the limitations of recent large-scale canopy height products in urban contexts. Int J Appl Earth Obs Geoinf 143:104791. https://doi.org/10.1016/j.jag.2025.104791

Du C, Ge S, Song P, et al (2025) Optimizing Urban Green Spaces for Vegetation-Based Carbon Sequestration: The Role of Landscape Spatial Structure in Zhengzhou Parks, China. Forests 16:679. https://doi.org/10.3390/f16040679

Duflot R, Avon C, Roche P, Bergès L (2018) Combining habitat suitability models and spatial graphs for more effective landscape conservation planning: An applied methodological framework and a species case study. J Nat Conserv

46:38–47. https://doi.org/10.1016/j.jnc.2018.08.005

Duncan JMA, Boruff B, Saunders A, et al (2019) Turning down the heat: An enhanced understanding of the relationship between urban vegetation and surface temperature at the city scale. Sci Total Environ 656:118–128. https://doi.org/10.1016/j.scitotenv.2018.11.223

ESA (2018) Copernicus Urban Atlas. https://land.copernicus.eu/local/urban-atlas/urban-atlas-2018. Accessed 13 Jul 2023

Eurostat (2020) Statistical Regions in the European Union and Partner Countries. NUTS and statistical regions 2021

Eurostat (2021) Applying the Degree of Urbanisation

FAO (2000) Global Forest Resources Assessment 2000, FRA 2000 Main Report. For Pap 140:479

Foltête J-C, Clauzel C, Vuidel G (2012) A software tool dedicated to the modelling of landscape networks. Environ Model Softw 38:316–327. https://doi.org/10.1016/j.envsoft.2012.07.002

Foltête J-C, Vuidel G, Savary P, et al (2021) Graphab: An application for modeling and managing ecological habitat networks. Softw Impacts 8:100065. https://doi.org/10.1016/j.simpa.2021.100065

Forman RTT (1995) Landscape mosaics. Ecol Landsc Reg 101:

Francini S, Chirici G, Chiesi L, et al (2024) Global spatial assessment of potential for new peri-urban forests to combat climate change. Nat Cities 1:286–294. https://doi.org/10.1038/s44284-024-00049-1

Fraucqueur L, Morin N, Masse A, et al (2019) A new Copernicus high resolution layer at pan-European scale: small woody features. In: Neale CM, Maltese A (eds) Remote Sensing for Agriculture, Ecosystems, and Hydrology XXI. SPIE, p 37

Frazier AE, Kedron P (2017) Landscape Metrics: Past Progress and Future Directions. Curr Landsc Ecol Reports 2:63–72. https://doi.org/10.1007/s40823-017-0026-0

Galpern P, Manseau M, Fall A (2011) Patch-based graphs of landscape connectivity: A guide to construction, analysis and application for conservation. Biol Conserv 144:44–55. https://doi.org/10.1016/j.biocon.2010.09.002

Gorelick N, Hancher M, Dixon M, et al (2017) Google Earth Engine: Planetary-scale geospatial analysis for everyone. Remote Sens Environ 202:18–27.

https://doi.org/10.1016/j.rse.2017.06.031

Gu D, Andreev K, E. Dupre M (2021) Major Trends in Population Growth Around the World. China CDC Wkly 3:604–613. https://doi.org/10.46234/ccdcw2021.160

Han L, Zhang R, Wang J, Cao S-J (2024) Spatial synergistic effect of urban green space ecosystem on air pollution and heat island effect. Urban Clim 55:101940. https://doi.org/10.1016/j.uclim.2024.101940

Hashemi R, Darabi H, Hashemi M, Wang J (2024) Graph theory in ecological network analysis: A systematic review for connectivity assessment. J Clean Prod 472:143504. https://doi.org/10.1016/j.jclepro.2024.143504

Herath P, Bai X, Jin H, Thatcher M (2024) Does the spatial configuration of urban parks matter in ameliorating extreme heat? Urban Clim 53:101756. https://doi.org/10.1016/j.uclim.2023.101756

Hesselbarth MHK, Sciaini M, Nowosad J, Hanss S (2024) Package ‘ landscapemetrics ’ Landscape Metrics for Categorical Map Patterns

Hesselbarth MHK, Sciaini M, With KA, et al (2019) landscapemetrics : an open-source R tool to calculate landscape metrics. Ecography (Cop) 42:1648–1657. https://doi.org/10.1111/ecog.04617

Huang X, Wang H, Shan L, Xiao F (2021) Constructing and optimizing urban ecological network in the context of rapid urbanization for improving landscape connectivity. Ecol Indic 132:108319. https://doi.org/10.1016/j.ecolind.2021.108319

Jutz S, Milagro-Pérez MP (2020) Copernicus: the European Earth Observation programme. Rev Teledetección. https://doi.org/10.4995/raet.2020.14346

Kim J, Kang W (2022) Assessing Green Roof Contributions to Tree Canopy Ecosystem Services and Connectivity in a Highly Urbanized Area. Land 11:1281. https://doi.org/10.3390/land11081281

Kim K, Serret H, Clauzel C, et al (2019) Spatio-temporal characteristics and predictions of the endangered leopard cat Prionailirus bengalensis euptilura road-kills in the Republic of Korea. Glob Ecol Conserv 19:e00673. https://doi.org/10.1016/j.gecco.2019.e00673

Kohler M, Blond N, Clappier A (2016) A city scale degree-day method to assess building space heating energy demands in Strasbourg Eurometropolis (France). Appl Energy 184:40–54. https://doi.org/10.1016/j.apenergy.2016.09.075

Kong F, Yin H, Nakagoshi N, Zong Y (2010) Urban green space network development for biodiversity conservation: Identification based on graph theory and gravity modeling. Landsc Urban Plan 95:16–27. https://doi.org/10.1016/j.landurbplan.2009.11.001

Konijnendijk CC (2023) Evidence-based guidelines for greener, healthier, more resilient neighbourhoods: Introducing the 3–30–300 rule. J For Res 34:821–830. https://doi.org/10.1007/s11676-022-01523-z

Kupfer JA (2012) Landscape ecology and biogeography. Prog Phys Geogr Earth Environ 36:400–420. https://doi.org/10.1177/0309133312439594

Lumia G, Praticò S, Di Fazio S, et al (2023) Combined use of urban Atlas and Corine land cover datasets for the implementation of an ecological network using graph theory within a multi-species approach. Ecol Indic 148:110150. https://doi.org/10.1016/j.ecolind.2023.110150

Maes J, Zulian G, Günther S, et al (2019) Enhancing Resilience Of Urban Ecosystems through Green Infrastructure (EnRoute) Final Report.

McGarigal K, Cushman SA, Ene E (2023) FRAGSTATS v4: Spatial pattern analysis program for categorical maps. https://www.fragstats.org/

McGarigal K, Marks BJ (1995) FRAGSTATS: spatial pattern analysis program for quantifying landscape structure. US Department of Agriculture, Forest Service, Pacific Northwest Research Station

Mu B, Tian G, Xin G, et al (2021) Measuring Dynamic Changes in the Spatial Pattern and Connectivity of Surface Waters Based on Landscape and Graph Metrics: A Case Study of Henan Province in Central China. Land 10:471. https://doi.org/10.3390/land10050471

Neyns R, Canters F (2022) Mapping of Urban Vegetation with High-Resolution Remote Sensing: A Review. Remote Sens 14:1031. https://doi.org/10.3390/rs14041031

Norton BA, Coutts AM, Livesley SJ, et al (2015) Planning for cooler cities: A framework to prioritise green infrastructure to mitigate high temperatures in urban landscapes. Landsc Urban Plan 134:127–138. https://doi.org/10.1016/j.landurbplan.2014.10.018

Pascual-Hortal L, Saura S (2006) Comparison and development of new graph-based landscape connectivity indices: towards the priorization of habitat patches and corridors for conservation. Landsc Ecol 21:959–967. https://doi.org/10.1007/s10980-006-0013-z

Raciti SM, Hutyra LR, Rao P, Finzi AC (2012) Inconsistent definitions of “urban” result in different conclusions about the size of urban carbon and nitrogen stocks.

Ecol Appl 22:1015–1035. https://doi.org/10.1890/11-1250.1

Sattler T, Pezzatti GB, Nobis MP, et al (2013) Selection of Multiple Umbrella Species for Functional and Taxonomic Diversity to Represent Urban. 28:414–426. https://doi.org/10.1111/cobi.12213

Saura S, Estreguil C, Mouton C, Rodríguez-Freire M (2011) Network analysis to assess landscape connectivity trends: Application to European forests (1990–2000). Ecol Indic 11:407–416. https://doi.org/10.1016/j.ecolind.2010.06.011

Saura S, Pascual-Hortal L (2007) A new habitat availability index to integrate connectivity in landscape conservation planning: Comparison with existing indices and application to a case study. Landsc Urban Plan 83:91–103. https://doi.org/10.1016/j.landurbplan.2007.03.005

Savary P, Clauzel C, Foltête J-C, et al (2024) Multiple habitat graphs: how connectivity brings forth landscape ecological processes. Landsc Ecol 39:168. https://doi.org/10.1007/s10980-024-01947-4

Savary P, Foltête J, Moal H, et al (2021) graph4lg: A package for constructing and analysing graphs for landscape genetics in R. Methods Ecol Evol 12:539–547. https://doi.org/10.1111/2041-210X.13530

Schindler S, von Wehrden H, Poirazidis K, et al (2015) Performance of methods to select landscape metrics for modelling species richness. Ecol Modell 295:107–112. https://doi.org/10.1016/j.ecolmodel.2014.05.012

Schwarz N (2010) Landscape and Urban Planning Urban form revisited — Selecting indicators for characterising European cities. Landsc Urban Plan 96:29–47. https://doi.org/10.1016/j.landurbplan.2010.01.007

Stroud S, Peacock J, Hassall C (2022) Vegetation-based ecosystem service delivery in urban landscapes: A systematic review. Basic Appl Ecol 61:82–101. https://doi.org/10.1016/j.baae.2022.02.007

Tarabon S, Godet C, Coskun T, Clauzel C (2022) Coupling spatial modeling with expert opinion approaches to restore multispecies connectivity of major transportation infrastructure. Landsc Urban Plan 221:104371. https://doi.org/10.1016/j.landurbplan.2022.104371

Turner MG, Gardner RH (2015) Landscape Ecology in Theory and Practice

United Nations (2018) The World’s Cities in 2018. World Urban Prospect 2018 Revis 34

Urban D, Keitt T (2001) Landscape Connectivity: A Graph-Theoretic Perspective. Ecology 82:1205. https://doi.org/10.2307/2679983

Uuemaa E, Antrop M, Roosaare J, et al (2009) Landscape metrics and indices: An overview of their use in landscape research. Living Rev Landsc Res 3:1–28. https://doi.org/10.12942/lrlr-2009-1

Uuemaa E, Mander Ü, Marja R (2013) Trends in the use of landscape spatial metrics as landscape indicators: A review. Ecol Indic 28:100–106. https://doi.org/10.1016/j.ecolind.2012.07.018

Villegas P, Gili T, Caldarelli G (2021) Emergent spatial patterns of coexistence in species-rich plant communities. Phys Rev E 104:034305. https://doi.org/10.1103/PhysRevE.104.034305

Villegas P, Gili T, Caldarelli G, Gabrielli A (2024) Evidence of scale-free clusters of vegetation in tropical rainforests. Phys Rev E 109:L042402. https://doi.org/10.1103/PhysRevE.109.L042402

Wu J (2004) Effects of changing scale on landscape pattern analysis : scaling relations. 125–138

Wulder MA, Loveland TR, Roy DP, et al (2019) Current status of Landsat program, science, and applications. Remote Sens Environ 225:127–147. https://doi.org/10.1016/j.rse.2019.02.015

Yan J, Zhou W, Han L, Qian Y (2018) Mapping vegetation functional types in urban areas with WorldView-2 imagery: Integrating object-based classification with phenology. Urban For Urban Green 31:230–240. https://doi.org/10.1016/j.ufug.2018.01.021

7. Statements & Declarations

7.1 Funding

Fundings for C.B. were supported by the Tuscany Region under the initiative “Green Transition – Advanced Training Projects with Research Grants” (CUP B53C23002970009), within the European Social Fund Plus (ESF+) 2021–2027 Regional Programme – Priority 4 ‘Youth Employment’ under the project “Advanced models for estimating carbon uptake by urban vegetation to support ecological transition policies”.

7.2 Competing Interests

The authors have no relevant financial or non-financial interests to disclose.

7.3 Author Contributions

Conceptualization, C.B., S.F., S.M., L.C., G.C, J.M, G.D.L., G.C.; Data curation, C.B., S.F., G.C.; Formal analysis, C.B.; Investigation, C.B., L.T., G.C., G.C., Methodology, C.B., G.C.; Project administration, S.M., G.C., G.C.; Writing—original draft, C.B. Writing—review and editing, C.B., S.F., L.C., S.M., L.T., G.C., J.M, E.V, G.D.A, G.D.L., G.C. All authors have read and agreed to the published version of the manuscript.

Leonardo Chiesi’s contribution is within the framework of the Jean Monnet Chair GREENSCAPE-EU, which is funded by the European Union. Views and opinions expressed are those of the author only and do not necessarily reflect those of the European Union or the EACEA). Neither the European Union nor EACEA can be held responsible for them

7.4 Data Availability

The data that support the findings of this study are available from the corresponding author upon reasonable request.

8. Annex

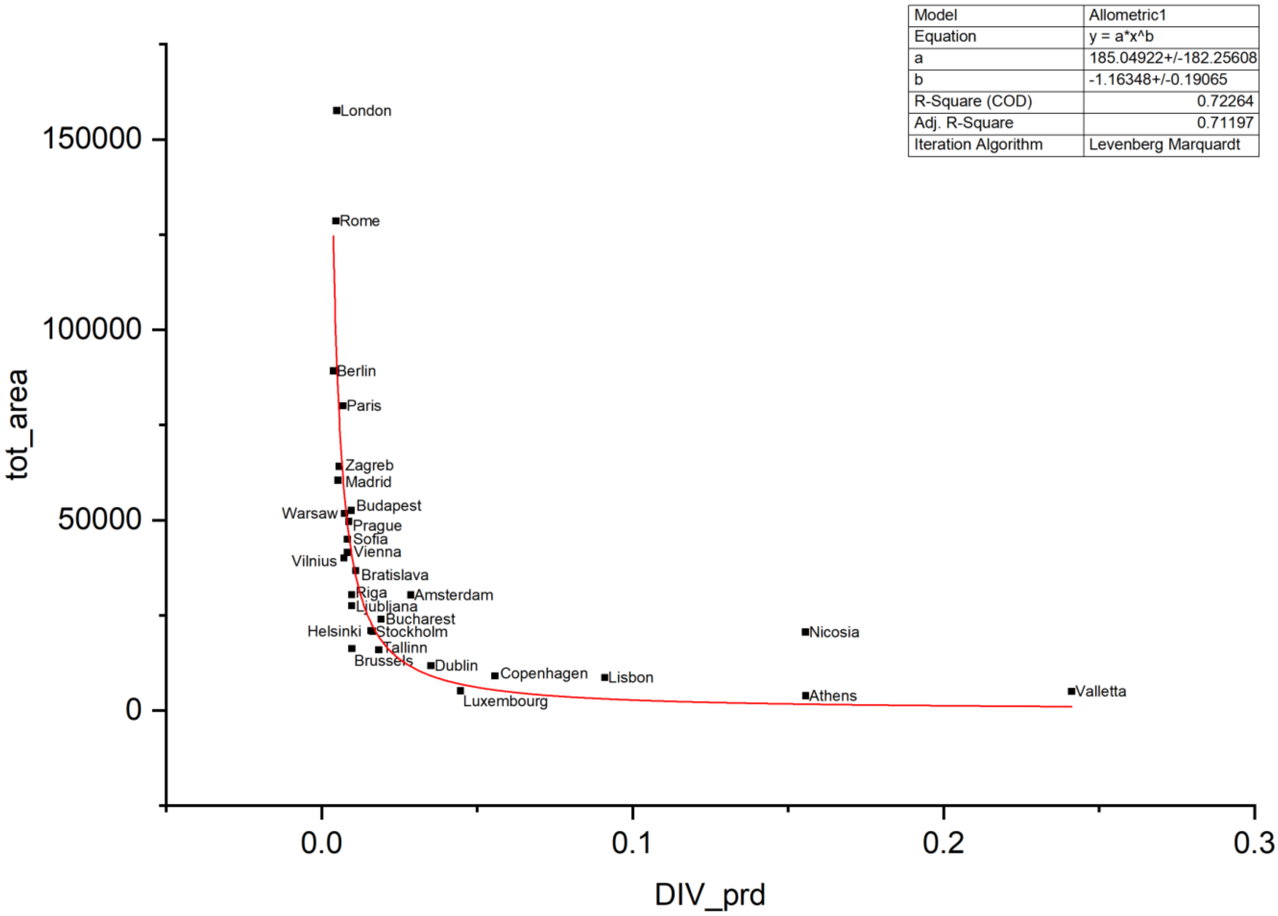

Fig. 10 The relationship between the total area covered by the area of UGS (tot_area) and DIV_prd.

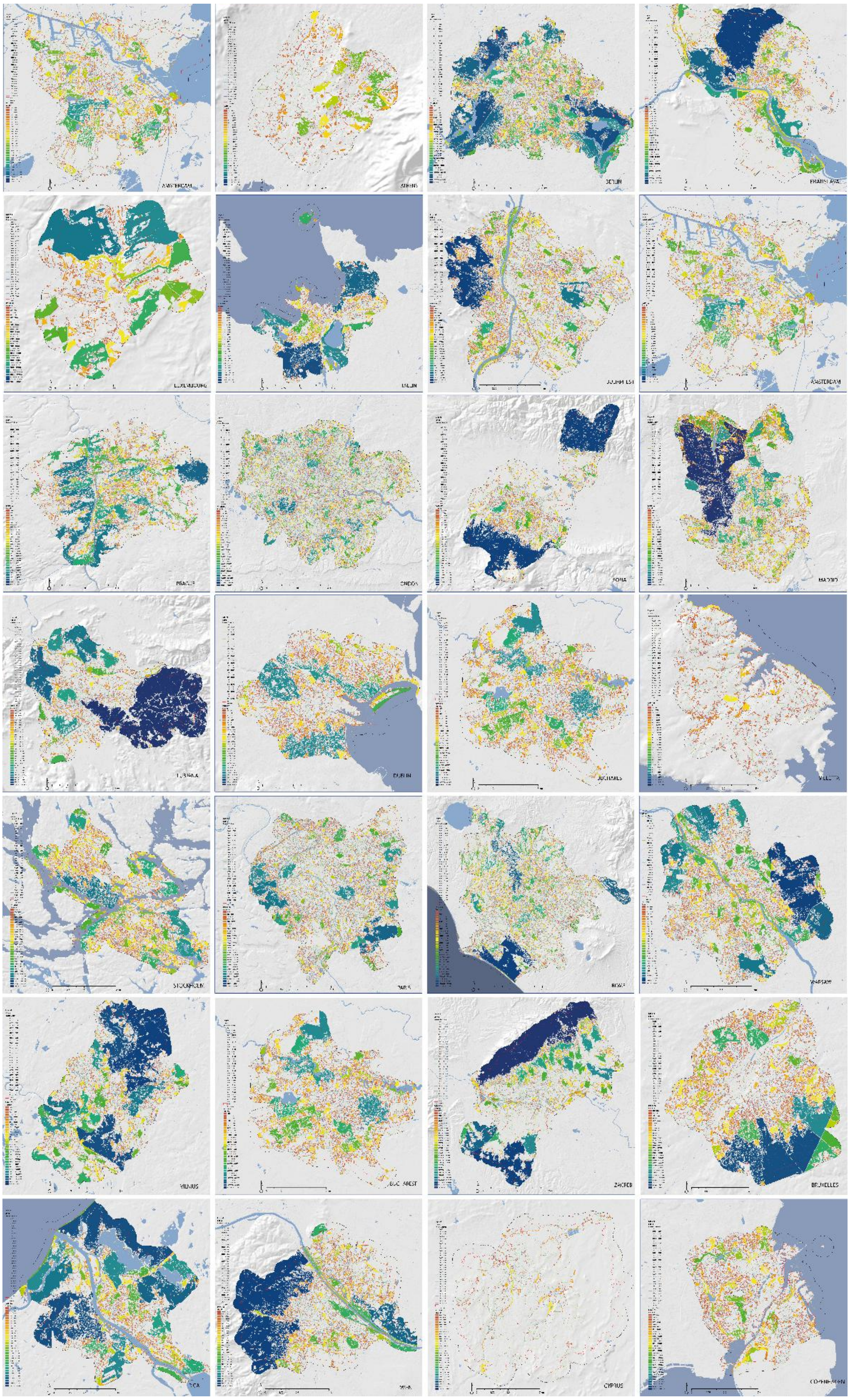

Fig.11 The result of the Graphab analysis for the 28 investigated European capitals with patches and the links between them

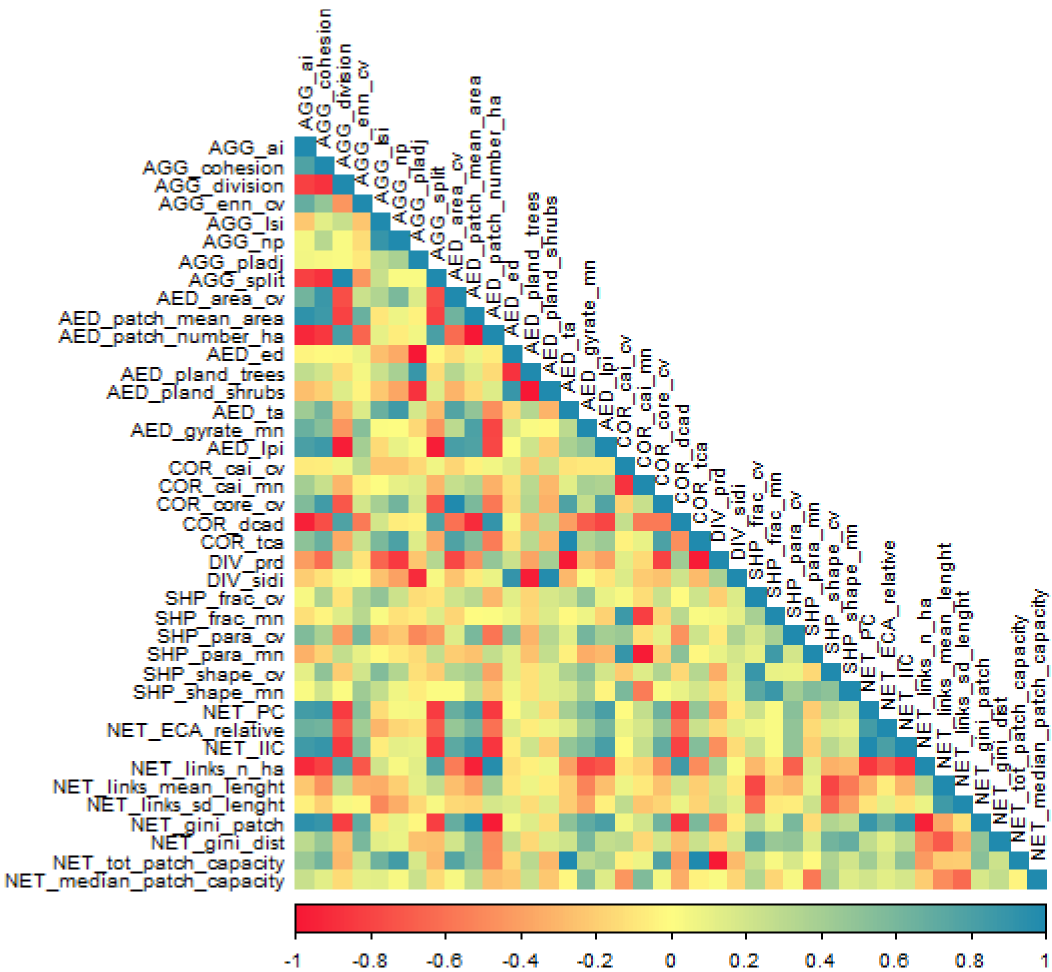

Fig. 12. Correlation among different landscape metrics (as reported in Table 2A)

Table 1A. Validation results for each Country's capital city, considering a 1km boundary. Overall Accuracy (OA), Producer's accuracy (PA), and User's Accurcay (UA) are reported as long as the LUCAS sampled points falling within each boundary (LUCAS_pt) and the number of True Positive (TP), True Negative (TN), False Positive (FP) and False Negative (FN).

City	**OA**	**PA**	**UA**	**LUCAS_pt**	**TP (n°)**	**TN (n°)**	**FP (n°)**	**FN (n°)**
Amsterdam	0.89	0.40	0.80	110	31	62	4	13
Athens	1.00	0.00	0.00	29	6	15	0	8
Berlin	0.85	0.67	0.93	58	13	39	5	1
Bratislava	0.89	0.81	0.89	83	1	69	13	0
Bruxelles	0.72	0.43	1.00	73	15	44	2	12
Bucharest	0.81	0.37	0.88	106	28	62	2	14
Budapest	0.79	0.50	0.70	11	1	8	0	2
Copenhagen	0.82	0.33	1.00	21	4	12	1	4
Dublin	0.64	0.11	1.00	11	0	11	0	0
Helsinki	0.87	0.85	0.91	144	37	68	10	29
Lisbon	1.00	1.00	1.00	60	29	23	3	5
Ljubljana	0.92	0.83	0.94	119	27	68	8	16
London	0.85	0.46	0.70	86	34	43	6	3
Luxembourg	0.77	0.50	0.67	48	7	31	3	7
Madrid	0.73	0.56	0.79	22	1	13	0	8
Nicosia	0.84	1.00	0.07	164	25	113	7	19

Paris	0.80	0.63	0.77	76	27	41	4	4
Prague	0.81	0.56	0.88	13	2	8	1	2
Riga	0.79	0.56	0.93	58	14	32	1	11
Rome	0.84	0.57	0.78	28	3	22	0	3
Sofia	0.90	0.93	0.72	61	4	50	1	6
Stockholm	0.88	0.77	0.92	53	18	27	0	8
Tallinn	0.76	0.50	0.80	14	2	12	0	0
Valletta	0.89	0.50	1.00	67	7	47	1	12
Vilnius	0.89	0.87	0.87	73	24	40	2	7
Warsaw	0.85	0.69	1.00	49	15	30	1	3
Wien	0.85	0.70	0.89	53	17	30	2	4
Zagreb	0.90	0.92	0.85	176	16	134	7	19

Table 2A. Landscape patterns and connectivity metrics calculated for each city

Group	Metric	Definition (Foltête et al., 2021; McGarigal et al., 2023)	Acronym
Aggregation (AGG)	aggregation index	The ratio of the observed number of like adjacencies to the maximum possible number of like adjacencies given the proportion of the landscape comprised of each patch type, given as a percentage	ai

Group	Metric	Definition (Foltête et al., 2021; McGarigal et al., 2023)	Acronym
	patch cohesion index	Measures the physical connectedness of the corresponding patch type at the landscape level. Patch cohesion increases as the patch type becomes more clumped or aggregated in its distribution	cohesion
	division index	The probability that two randomly chosen pixels in the landscape are not situated in the same patch	division
	Euclidean nearest neighbor distance (coefficient of variation)	The coefficient of variation of the edge-to-edge distance to the nearest neighboring patch of the same class	enn_cv
	landscape shape index	A standardized measure of patch compactness that adjusts for the size of the patch. As lsi increases, the patches become increasingly disaggregated	lsi
	Number of patches	The total number of patches in the landscapes	np
	Percentage of like adjacencies	It calculates the frequency of how often patches of different classes i (focal class) and k are next to each other	pladj
	splitting index	It describes the number of patches if all patches the landscape were divided into equally sized patches	split
Area and edge (AED)	Patch area (coefficient of variation)	The metric summarises the landscape as the coefficient of variation of the size of all patches in the landscape.	area_cv

Group	Metric	Definition (Foltête et al., 2021; McGarigal et al., 2023)	Acronym
	Patch area (mean)	The metric summarises the landscape as the mean size of all patches in the landscape.	Patch_mean_area
	Patch number	The total number of patches per hectare	Patch_number_ha
	Edge density	The sum of the lengths (m) of all edge segments in the landscape, divided by the total landscape area (ha)	ed
	Percentage of landscape belonging to class i	The percentage of the total landscape belonging to class "trees" and/or "shrubs"	pland_trees pland_shrubs
	Total area	The total area of all patches in the landscape	ta
	Radius of gyration (mean)	It summarises the landscape as the mean of the radius of gyration of all patches in the landscape	gyrate_mn
	Largest patch index	The area (ha) of the largest patch in the landscape divided by the total landscape area (ha) multiplied by 100 to convert to a percentage	lpi
Core area (COR)	Core area index (coefficient of variation)	The metric summarizes the landscape as the coefficient of variation of the core area index (i.e, the percentage of total core area (tca) to total area) of all patches in the landscape	cai_cv
	core area index (mean)	The mean of the core area index of all patches in the landscape	cai_mn

Group	Metric	Definition (Foltête et al., 2021; McGarigal et al., 2023)	Acronym
	core area (coefficient of variation)	Coefficient of variation of the core area (all cells that have no neighbor with a different value than themselves (rook's case)) of each patch in the landscape	core_cv
	disjunct core area density	It equals the number of disjunct core areas per 100 ha relative to the total area. A disjunct core area is a “patch within the patch” containing only core cells (if the cell has no neighbor with a different value than itself)	dcad
	total core area	It equals the sum of the core areas of all patches in the landscape	tca
Diversity (DIV)	patch richness density	The number of different patch types (trees and shrubs) present within the landscape boundary, divided by the total landscape area	prd
	Simpson's diversity index	The probability that any 2 pixels selected at random would be of different patch types (trees and shrubs)	sidi
Shape (SHP)	fractal dimension index (coefficient of variation)	Coefficient of variation of the fractal dimension index of all patches in the landscape, which is based on the patch perimeter and the patch area and describes the patch complexity	frac_cv
	fractal dimension index (mean)	The mean value of the fractal dimension index of all patches in the landscape	frac_mn

Group	Metric	Definition (Foltête et al., 2021; McGarigal et al., 2023)	Acronym
	perimeter-area ratio (coefficient of variation)	The coefficient of variation of the perimeter-area ratio of all patches in the landscape, which describes the patch complexity in a straightforward way	para_cv
	perimeter-area ratio (mean)	The mean of the perimeter-area ratio, which describes the patch complexity in a straightforward way	para_mn
	shape index (coefficient of variation)	Weighting patches according to their size, in contrast to lsi, in which the total length of the edge is compared to a landscape with a standard shape (square) of the same size and without any internal edge	shape_cv
	shape index (mean)	It describes the ratio between the actual perimeter of the patch and the square root of the patch area (mean of all patches in the landscape)	shape_mn
Network (NET)	Probability of connectivity	The probability that two individuals, randomly placed within the landscape, fall into interconnected habitats	PC
	Equivalent Connected Area (relative)	The size of the single habitat patch, maximally connected, that would provide the same value of PC as the actual habitat pattern in the landscape, standardized over the total landscape capacity (area)	ECA_relative

Group	Metric	Definition (Foltête et al., 2021; McGarigal et al., 2023)	Acronym
	Integral Index of Connectivity	The probability that individuals randomly located in the landscape within a patch can access each other	IIC
	Number of links per hectare	Number of links equal or shorter than 200 m per hectare, considering the whole landscape	links_n_ha
	Mean of link length	Mean length of links equal or shorter than 200 m	links_mean_lenght
	Standard deviation of link length	Standard deviation of length of links equal or shorter than 200m, considering the whole landscape	links_sd_lenght
	Gini on patch capacity	Gini index on patch capacity (area)	gini_patch
	Gini on patch distance	Gini index on links' length	gini_dist
	Total patch capacity	Sum of the total patch capacity (area)	tot_patch_capacity
	Median patch capacity	Median of the total patch capacity (area)	median_patch_capacity

Table 3A. Urban land cover based on the European Map of Vegetation, calculated for each city as an absolute value (in km^2) and percentage of the total area. The categories are non-vegetated areas (Non Veg), trees, shrubs, grass, and total vegetation (Veg) as the sum of trees, shrubs and grass

City	**Non Veg (km^2)**	**Trees (km^2)**	**Shrubs (km^2)**	**Grass (km^2)**	**Tot. area (km^2)**	**Veg (km^2)**	**Non Veg (%)**	**Trees (%)**	**Shrubs (%)**	**Grass (%)**	**Veg (%)**
Amsterdam	169.77	60.59	0.38	72.67	303.4	133.64	55.95	19.97	0.13	23.95	44.05
Athens	31.41	7.34	0	0.24	39	7.59	80.54	18.83	0	0.63	19.46
Berlin	386.04	432.74	1.59	71.49	891.86	505.82	43.28	48.52	0.18	8.02	56.72
Bratislava	96.2	146.2	1.53	123.58	367.51	271.31	26.18	39.78	0.42	33.63	73.83
Brussels	87.25	69.57	0	5.65	162.47	75.22	53.7	42.82	0	3.48	46.3
Bucharest	122.17	79.35	0.67	37.38	239.57	117.4	51	33.12	0.28	15.6	49.01
Budapest	265.71	165.16	0.21	94.11	525.19	259.48	50.59	31.45	0.04	17.92	49.41
Copenhagen	59.91	20.17	1.72	8.96	90.76	30.85	66.01	22.23	1.89	9.87	33.99
Dublin	68.49	39.24	2.4	7.56	117.68	49.19	58.2	33.34	2.04	6.42	41.8
Helsinki	91.81	95.37	0.41	20.83	208.42	116.61	44.05	45.76	0.2	9.99	55.95
Lisbon	63.53	17.91	0.58	4.46	86.47	22.94	73.47	20.71	0.67	5.16	26.53
Ljubljana	58.44	142.49	0.9	73.22	275.06	216.61	21.25	51.81	0.33	26.62	78.75
London	937.73	364.97	0.66	272.37	1575.73	637.99	59.51	23.16	0.04	17.29	40.49
Luxembourg	21.28	20.85	0.23	9.38	51.74	30.46	41.13	40.3	0.44	18.13	58.87

Madrid	200.78	262.63	42.16	99.43	604.99	404.21	33.19	43.41	6.97	16.43	66.81
Nicosia	152.63	6.5	0	47.02	206.14	53.51	74.04	3.15	0	22.81	25.96
Paris	552.91	210.85	0.01	36.57	800.34	247.43	69.08	26.35	0	4.57	30.92
Prague	162.22	179.7	1.42	153.12	496.46	334.24	32.68	36.2	0.29	30.84	67.32
Riga	130.96	146.87	2.51	23.82	304.15	173.19	43.06	48.29	0.82	7.83	56.94
Rome	340.95	346.7	3.14	595.17	1285.96	945.01	26.51	26.96	0.24	46.28	73.49
Sofia	127.39	179.18	0.06	143.39	450.02	322.63	28.31	39.82	0.01	31.86	71.69
Stockholm	112.58	85.45	0.07	11.89	209.98	97.4	53.61	40.7	0.03	5.66	46.39
Tallinn	67.2	79.06	1.1	12.11	159.46	92.27	42.14	49.58	0.69	7.59	57.86
Valletta	31.97	4	2.03	12.23	50.23	18.26	63.64	7.96	4.05	24.35	36.36
Vienna	171.28	179.03	0.12	64.41	414.84	243.56	41.29	43.16	0.03	15.53	58.71
Vilnius	116.39	197.55	0.66	85.98	400.58	284.19	29.06	49.32	0.17	21.46	70.95
Warsaw	215.48	218.81	0.41	82.53	517.23	301.75	41.66	42.3	0.08	15.96	58.34
Zagreb	151.66	273.15	2.39	214.09	641.3	489.63	23.65	42.59	0.37	33.38	76.35

Table 4A. Aggregation metrics (AGG) calculated in the 28 European Capitals

City	AGG_ai	AGG_cohesion	AGG_division	AGG_enn_cv	AGG_lsi	AGG_np	AGG_pladj	AGG_split
Amsterdam	87.35	98.26	0.98	117.7	106.45	3893	99.94	62.19
Athens	88.02	97.32	0.97	112.32	43.72	919	99.82	37.73
Berlin	91.98	99.69	0.94	250.66	186.51	10310	99.94	17.13
Bratislava	95.02	99.49	0.83	305.81	67.43	2868	99.85	6.06
Brussels	91.95	99.53	0.83	75.95	82.48	3159	100	6.05
Bucharest	89.28	99.1	0.97	214.43	110.37	4130	99.92	31.02
Budapest	90.97	99.34	0.92	90.19	131.79	8680	99.98	12.52
Copenhagen	86.58	97.15	0.99	105.87	79.98	2482	99.45	109.58
Dublin	86.07	99.19	0.94	81.73	106	3045	99.97	15.69
Helsinki	91.2	98.85	0.96	437.48	98.15	3101	99.94	28.29
Lisbon	90.53	98.02	0.92	131.91	44.92	1233	99.73	13.05
Ljubljana	96.34	99.8	0.67	265.91	53.26	2641	99.91	3
London	87.46	98.24	1	105.24	255.24	27276	99.99	233.68
Luxembourg	95.37	99.24	0.87	270.63	31.8	726	99.94	7.93
Madrid	90.38	99.8	0.8	151.4	172.45	9347	98.13	5.03
Nicosia	79.14	93.76	0.99	180.7	53.57	1048	100	83.81
Paris	90.09	98.88	0.98	85.69	169.42	15093	100	40.08
Prague	92.09	99.59	0.93	228.13	120.32	5167	99.91	14.39

Riga	93.76	99.73	0.9	266.91	89.9	2336	99.85	10.38
Rome	90.81	99.42	0.95	140.53	191.23	13519	99.9	19.61
Sofia	95.04	99.74	0.74	322.42	78.13	4833	99.99	3.8
Stockholm	90.95	98.89	0.98	177.09	102.73	4040	99.98	44.81
Tallinn	92.93	99.73	0.82	414.71	74.25	1926	99.87	5.43
Valletta	81.48	92.38	0.99	118.95	52.49	1417	98.33	140.15
Vienna	93.9	99.83	0.68	246.85	96.14	4394	99.99	3.11
Vilnius	95.37	99.7	0.88	252.02	78.34	4031	99.97	8.57
Warsaw	92.23	99.34	0.94	273.08	129.41	8903	99.98	16.31
Zagreb	96.79	99.73	0.79	207.62	60.28	3959	99.86	4.7

Table 5A. Area and Edge metrics (AED) calculated in the 28 European Capitals

City	AED_area_cv	AED_patch_mean_area	AED_patch_number_ha	AED_ed	AED_pland_trees	AED_pland_shrubs	AED_ta	AED_gyrate_mn	AED_lpi
Amsterdam	784.98	1.8	0.56	1.03	0.2	0	6991.58	43.1	9.1
Athens	483.56	1.4	0.72	3.11	0.19	0	1285.1	36.29	7.55
Berlin	2451.61	5.23	0.19	1.11	0.49	0	53967.02	47.34	17.54
Bratislava	2173.58	6.37	0.16	2.81	0.4	0	18269.68	54.17	38.15
Brussels	2283.22	3.25	0.31	0	0.43	0	10276.97	44.52	39.05
Bucharest	1149.62	2.54	0.39	1.47	0.33	0	10491.44	42.85	10.86
Budapest	2631.35	2.42	0.41	0.37	0.31	0	21040.66	42.32	27.28
Copenhagen	465.4	1.45	0.69	9.45	0.22	0.02	3590.16	42.3	3.41

Dublin	1389.9	1.87	0.53	0.54	0.33	0.02	5695.3	41.55	15.94
Helsinki	1042.44	3.96	0.25	1.02	0.46	0	12274.73	52.76	15.78
Lisbon	967.27	1.78	0.56	4.89	0.21	0.01	2197.46	40.53	22.36
Ljubljana	2964.91	7.88	0.13	1.7	0.52	0	20823.81	46.03	56.13
London	1075.77	1.51	0.66	0.18	0.23	0	41169.81	39.31	3.46
Luxembourg	952.1	6.18	0.16	1.03	0.4	0	4484.74	55.52	28.59
Madrid	4310.62	4.09	0.24	34.33	0.43	0.07	38227.11	45.32	44.28
Nicosia	339.35	0.61	1.63	0	0.03	0	642.69	34.47	6.06
Paris	1938	1.92	0.52	0.01	0.26	0	28930.91	39.17	11.26
Prague	1892.41	4.45	0.22	1.69	0.36	0	22996.02	48.84	22.49

Riga	1497.22	8.9	0.11	2.84	0.48	0.01	20782.7	54.92	19
Rome	2623.64	3.2	0.31	1.73	0.27	0	43303.55	48.91	20.12
Sofia	3566.51	5.02	0.2	0.15	0.4	0	24253.57	40.39	38.1
Stockholm	944.36	3.14	0.32	0.32	0.41	0	12686.39	49.43	10.41
Tallinn	1881.65	5.67	0.18	2.44	0.5	0.01	10919.45	46.63	34.93
Valletta	301.94	0.59	1.71	27.56	0.08	0.04	829.32	30.87	4.2
Vienna	3757.39	5.54	0.18	0.16	0.43	0	24350.02	47.51	55.69
Vilnius	2167.04	6.97	0.14	0.62	0.49	0	28094.66	47.38	28.48
Warsaw	2334.43	3.07	0.33	0.31	0.42	0	27368.06	40.77	21.51
Zagreb	2899.57	9	0.11	2.77	0.43	0	35643.88	49.85	40.53

Table 6A. Core area (COR) and diversity (DIV) metrics calculated in the 28 European Capitals

City	COR_cai_cv	COR_cai_mn	COR_core_cv	COR_dcad	COR_tca	DIV_prd	DIV_sidi
Amsterdam	46.85	33.94	933.77	150.8	4528.28	0.03	0.01
Athens	47.03	35.86	559.99	158.2	861.38	0.16	0.08
Berlin	36.97	40.3	2768.54	86.23	41359.85	0	0.01
Bratislava	37.39	43.16	2417.79	37.02	15640.9	0.01	0.02
Brussels	32.77	44.55	2587.35	66.88	7890.67	0.01	0
Bucharest	32.31	42.75	1309.38	95.94	7205.14	0.02	0.02
Budapest	31.49	43.35	3077.78	80.54	15707.24	0.01	0
Copenhagen	32.23	41.23	554.7	137.99	2223.93	0.06	0.09
Dublin	41.02	34.19	1596.34	182.94	3485.62	0.04	0.09
Helsinki	59.98	33.98	1244.79	96.2	9319.92	0.02	0.01
Lisbon	40.57	40.79	1180.48	100.62	1594.11	0.09	0.13
Ljubljana	40.49	39.55	3136.36	28.01	18611.43	0.01	0.01
London	46.26	34.49	1329.66	145.45	27054.44	0	0
Luxembourg	36.19	45.7	1027.1	31.51	3885.77	0.04	0.01
Madrid	59.56	31.1	4910.04	115.87	27659.92	0.01	0.27
Nicosia	66.81	24.67	483.73	348.54	294.9	0.16	0
Paris	30.62	42.35	2369.86	101.37	20918.63	0.01	0
Prague	33.77	43.2	2070.96	51.83	17693.87	0.01	0.01

Riga	41.33	39.04	1584.08	54.85	17031.45	0.01	0.03
Rome	38.03	40.81	3188.05	73.98	31909.45	0	0.02
Sofia	47.4	35.6	3886.42	44.19	20855.4	0.01	0
Stockholm	51.82	36.95	1043.75	89.1	9529.31	0.02	0
Tallinn	52.62	34.36	1998.25	72.2	8724.25	0.02	0.02
Valletta	57.76	29.58	442.66	281.07	419.65	0.24	0.45
Vienna	32.58	43.76	4092.91	43.66	20003.58	0.01	0
Vilnius	38.84	41.29	2309.5	35.43	24369.54	0.01	0.01
Warsaw	57.37	31.14	2692.34	90.18	21515.5	0.01	0
Zagreb	62.11	34.91	3073.01	23.49	32407.99	0.01	0.02

Table 7A. Shape (SHP) metrics calculated in the 28 European Capitals

City	SHP_frac_cv	SHP_frac_mn	SHP_para_cv	SHP_para_mn	SHP_shape_cv	SHP_shape_mn
London	4.55829	1.099304	29.37656	0.105548	48.22349	1.620655
Rome	5.150586	1.092584	30.01283	0.089112	64.67979	1.648261
Berlin	5.351137	1.095962	29.48761	0.090317	83.5647	1.700307
Paris	4.519565	1.083671	25.21146	0.088327	46.22801	1.526005
Zagreb	4.311407	1.105608	38.83555	0.104971	40.01334	1.659287
Madrid	5.682219	1.11429	52.53453	0.117068	79.31366	1.820272
Budapest	4.714273	1.082724	27.61176	0.086604	50.18052	1.538545
Warsaw	4.834903	1.113004	31.40116	0.112245	47.56531	1.726225
Prague	5.073451	1.085507	31.15479	0.085513	72.07524	1.608124
Sofia	4.720795	1.096329	30.69161	0.102381	47.80409	1.610705
Vienna	4.938421	1.085153	28.17366	0.084293	63.59218	1.585153
Vilnius	4.648738	1.08743	31.15439	0.089988	53.3317	1.572157
Bratislava	5.235227	1.093287	33.8654	0.086953	56.27718	1.660243
Riga	5.374511	1.106101	38.01724	0.095199	84.94071	1.792029
Amsterdam	5.281038	1.103448	28.61367	0.10464	56.36764	1.69678
Ljubljana	4.780971	1.087387	33.21776	0.09205	48.89887	1.561911
Bucharest	5.154363	1.081109	27.82255	0.08627	70.08946	1.572379
Stockholm	5.061944	1.109843	35.52912	0.101912	54.06514	1.758397

Helsinki	5.422711	1.128828	37.08175	0.109385	57.94745	1.943617
Nicosia	4.641932	1.120589	27.31582	0.12654	35.36626	1.709601
Brussels	4.620311	1.084916	29.31235	0.083795	55.09956	1.561532
Tallinn	5.199241	1.112635	32.68229	0.107607	70.17051	1.786362
Dublin	5.320235	1.106855	26.54715	0.104948	69.88132	1.729443
Copenhagen	4.916929	1.09064	30.02082	0.089645	48.92141	1.598796
Lisbon	4.289724	1.084375	32.21691	0.089194	35.94261	1.514516
Luxembourg	4.553345	1.088218	36.74546	0.083304	43.15458	1.586448
Valletta	4.093757	1.098221	29.649	0.114914	28.00114	1.541401
Athens	4.505419	1.093161	30.2926	0.103701	44.50046	1.567807

Table 8A. Network (NET) metrics calculated in the 28 European Capitals

City	NET_PC	NET_ECA_relative	NET_IIC	NET_links_n_ha	NET_links_mean_lenght	NET_links_sd_lenght	NET_gini_patch	NET_gini_dist	NET_tot_patch_capacity	NET_median_patch_capacity
Amsterdam	0	0.1	0	1.25	69.98	54.12	0.83	0.6	7008.72	0.28
Athens	0.01	0.38	0.01	1.32	79.88	58.27	0.8	0.49	1290.14	0.26
Berlin	0.02	0.31	0.02	0.72	54.4	48.32	0.92	0.6	51153.99	0.28
Bratislava	0.03	0.37	0.02	0.47	59.56	51.44	0.93	0.67	17574.5	0.32
Brussels	0.05	0.49	0.04	1.04	64.37	49.56	0.88	0.53	9665.55	0.32
Bucharest	0.01	0.23	0.01	1.32	65.26	52.56	0.84	0.59	9680.22	0.28
Budapest	0.01	0.22	0.01	1.35	68.96	52.52	0.85	0.54	19473.74	0.28
Copenhagen	0	0.2	0	2.32	67.33	51.45	0.75	0.56	3208.19	0.29
Dublin	0.03	0.39	0.02	1.37	62.77	50.98	0.84	0.55	5704.45	0.29
Helsinki	0.02	0.39	0.01	0.65	60.64	50.99	0.9	0.63	12298.49	0.31
Lisbon	0.01	0.16	0	1.45	78.27	58.36	0.81	0.52	2037.23	0.26
Ljubljana	0.13	0.82	0.1	0.34	73.6	56.81	0.96	0.55	20304.92	0.26
London	0	0.08	0	1.63	74.62	53.45	0.81	0.52	41429.48	0.28

Luxembourg	0.1	0.87	0.06	0.45	70.46	53.73	0.93	0.55	4312.68	0.33
Madrid	0.06	0.47	0.04	0.75	46.72	51.56	0.91	0.69	36404.75	0.24
Nicosia	0	0.01	0	2.46	84.66	59.8	0.65	0.56	656.78	0.2
Paris	0.01	0.18	0.01	1.66	74.48	53.7	0.83	0.52	26625.9	0.27
Prague	0.02	0.26	0.01	0.76	56.89	49.77	0.9	0.64	21484.93	0.31
Riga	0.11	0.77	0.08	0.41	58.95	52.53	0.95	0.62	20003.12	0.28
Rome	0.03	0.43	0.03	0.92	74.1	56.68	0.88	0.57	40200.73	0.28
Sofia	0.09	0.9	0.08	0.51	69.94	54.29	0.94	0.62	24218.79	0.28
Stockholm	0.02	0.46	0.02	0.93	54.71	47.58	0.87	0.63	12707.58	0.31
Tallinn	0.03	0.78	0.03	0.46	60.47	52.95	0.94	0.69	10911.03	0.28
Valletta	0	0.07	0	3.77	70.9	58.84	0.62	0.56	847.92	0.22
Vienna	0.08	0.55	0.06	0.58	63.83	52.98	0.92	0.59	23392.74	0.32
Vilnius	0.06	0.6	0.05	0.42	70.55	54.99	0.95	0.56	27173.43	0.25
Warsaw	0.05	0.43	0.04	0.94	65.47	51.78	0.9	0.55	27378.63	0.26
Zagreb	0.05	0.58	0.05	0.2	73.92	57.58	0.96	0.59	35666.69	0.27